

## Review

# 3D printing of polymer composites: Materials, processes, and applications

Soyeon Park,<sup>1</sup> Wan Shou,<sup>2,3,4,\*</sup> Liane Makatura,<sup>2,3</sup> Wojciech Matusik,<sup>2,3</sup> and Kun (Kelvin) Fu<sup>1,5,\*</sup>

## SUMMARY

Additive manufacturing (AM) (also known as 3D printing) has enabled the customized fabrication of objects with complex geometries and functionalities in mechanical and electrical properties. AM technologies commonly use polymers and composites and have been advancing in a variety of industrial and emerging applications. Despite recent progress in 3D printing of polymer composites, many challenges, such as the suboptimal quality of manufactured products and limited material available for 3D printing, need to be addressed for the broad adoption of additively manufactured polymer composites. This review first provides a brief history of AM technologies along with 3D printing polymers. Subsequently, we discuss the state-of-the-art for the design of polymers and filling materials, the principles of AM processes, and emerging applications of 3D printed polymer and composites. Finally, we share our outlook of potential problems and challenges presented in AM of polymer composites, which might lead to future research directions.

## INTRODUCTION

Additive manufacturing (AM), also known as 3D printing, usually builds 3D objects by adding materials layer upon layer to form the desired shape. AM is agile and can directly create complex shapes from a digital model, which differs from conventional manufacturing techniques such as milling and molding. With traditional manufacturing processes, whenever making a new component or changing a part design, they require a new tool, mold, or jig. On the other hand, in 3D printing, it does not need any physical changes of equipment or machine after designing the product in software. Thus, 3D printing techniques are changing time-consuming and labor-intensive manufacturing processes. Furthermore, they reduce material waste compared with subtractive manufacturing approaches. Together with other significant advantages, including flexibility in complex geometry design, tailored property, and customization, AM gives new insights not only in the manufacturing field but also in diverse industries such as biomedicine, electrical energy storage, electronics, and robotics.

Different types of 3D printers use different materials (such as polymer, ceramic, metal, and composites). For example, one commonly used 3D printer, fused filament fabrication, uses polymers and polymer-based composites with the addition of different types of fillers, including metal and ceramic nanoparticles. Among various materials, a polymer is one of the most widely used feedstocks in almost all types of 3D printing methods except for directed-energy deposition. Depending on the printing methods and applications, different types of polymers, including thermoplastics and photopolymers, can be tailored to fit the manufacturing process.

## Progress and potential

The development of polymers is always closely linked with the advancement of polymer manufacturing and processing. Since the origination of additive manufacturing (AM) in the 1980s, there has been rapid development with increasing interest in AM technologies for polymers and their composite due to the advantages of high efficiency, resolution, and customization. However, AM requires certain conditions of polymers and composites (e.g., shape, physical, and rheological properties), and it offers limited application of AM in diverse industries. This paper provides directions to overcome these challenges by introducing the working principles of AM techniques for polymers and polymer composites and suggesting how to design and select polymers and filling materials for structural and functional applications. Finally, we share our perspective of potential problems and challenges in printing polymer composites as a guideline for the future development of polymer materials/chemistry and AM technologies.



However, the 3D printed polymer products are rarely used for structural and functional parts because they have unsatisfied mechanical properties and exhibit electrically and thermally insulating behavior in general. Hence, 3D printing for polymer composites has been widely researched to overcome these limitations in mechanical performance by adding reinforcement materials such as nanoparticles and short or continuous fibers. Moreover, if functional materials, such as metal or metal oxide and living cells, are added in the polymers, the 3D printed polymer composites can perform better than conventional composites in specific functional applications. Recently, many studies about 3D printing using polymer composites, such as architected composite materials,<sup>1,2</sup> and shape-morphing composites,<sup>3</sup> are emerging. Meanwhile, AM is transforming from rapid prototyping to real production. Therefore, it is urgent to review the recent development of 3D printing of polymer composites and discuss existing challenges and opportunities for the future development of polymer composites and 3D printing technologies.

In this paper, we review advances of AM technologies along with polymer materials, physical and chemical properties of polymers, and filling materials for structural and functional applications. First, we discuss representative 3D printers and their working principles for polymers and polymer composites. Subsequently, we elaborate on emerging applications using AM (3D printing), including structural and functional applications in biology, electrical energy storage, electronics, and robotics. Finally, we will discuss the challenges and opportunities for AM of polymer composites.

## EVOLUTION OF POLYMER 3D PRINTING

### History of polymer 3D printing

The timeline of 3D printing, along with the development of polymer materials, is summarized in [Figure 1](#). The development of feedstock materials, especially polymers, is indispensable in the invention of 3D printing. Most polymers, including polyamides, polylactic acid (PLA), and epoxy, were synthesized and developed during the 1920s and 1940s.<sup>4</sup> The fundamental concepts of AM were studied more than 50 years ago. The 1980s and 1990s were the decades of the birth and growth of 3D printing. The first 3D printing method, stereolithography, was commercialized in 1987. Other 3D printing techniques such as fused filament fabrication (FFF) and selective laser sintering (SLS) were also invented in this period.<sup>5</sup> In the late 1990s, most of the first versions of 3D printing techniques emerged and evolved rapidly, attributed to the progress of computer technologies. 3D printing techniques started to be explored widely in industries including medical and aerospace fields in the early 2000s. At the same time, many patents for the earlier versions of 3D printing techniques expired, and many companies started to make their brands of 3D printers, making 3D printers accessible to the general public. After 2010, widespread access to 3D printing techniques has led to advanced printing techniques with enhanced accuracy, precision, and speed. In the early stages, AM techniques mainly adopted existing polymer materials and made them suitable for AM. Nowadays, increasing attention is being paid to the development of 3D printing polymers, namely, polymer development for 3D printing. With the fast development of high-performance 3D printing materials (e.g., smart polymers as well as advanced engineering plastics), AM has become a fundamental process and led to the new industrial revolution in various fields. For instance, newly designed polymers, such as shape memory polymers (SMPs),<sup>6–9</sup> smart hydrogels,<sup>3,10,11</sup> and liquid crystal polymers (LCPs) and liquid crystal elastomers (LCEs),<sup>12–15</sup> have led to a new manufacturing paradigm including 4D printing and give industries a chance to produce novel smart devices,<sup>16</sup> robots,<sup>17</sup> and biomedical products.<sup>18</sup> Currently, 3D printing is undergoing a transition from prototyping to end-use products, which

<sup>1</sup>Department of Mechanical Engineering, University of Delaware, Newark, DE 19716, USA

<sup>2</sup>Computer Science and Artificial Intelligence Laboratory, Massachusetts Institute of Technology, Cambridge, MA 02139, USA

<sup>3</sup>Electrical Engineering and Computer Science Department, Massachusetts Institute of Technology, Cambridge, MA 02139, USA

<sup>4</sup>Department of Mechanical Engineering, University of Arkansas, Fayetteville, AR 72701, USA

<sup>5</sup>Center for Composite Materials, University of Delaware, Newark, DE 19716, USA

\*Correspondence: [wanshou@mit.edu](mailto:wanshou@mit.edu) (W.S.), [kfu@udel.edu](mailto:kfu@udel.edu) (-g.F.)

<https://doi.org/10.1016/j.matt.2021.10.018>

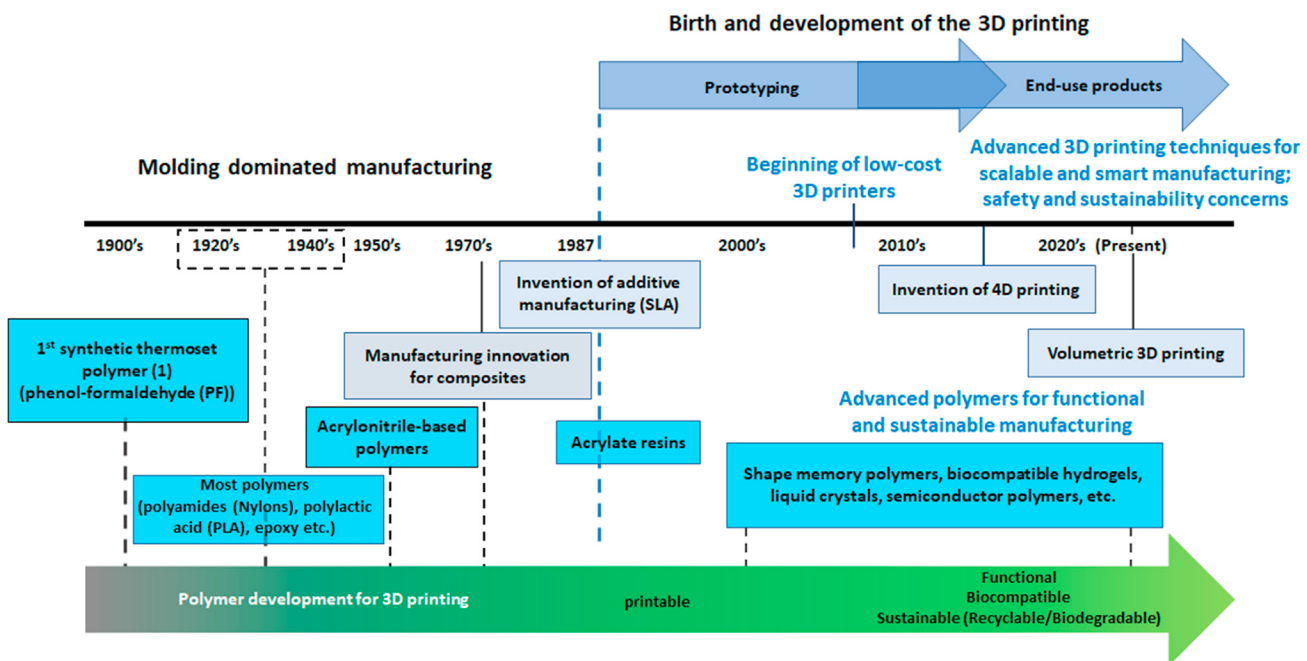


**Figure 1. 3D Printing history and polymer development for 3D printing: transitioning from rapid prototyping toward scalable and customizable production**

Polymers have evolved from being printable (to meet the requirement of prototyping) to be more functional, biocompatible, and sustainable (to meet the requirements for end-use products).

will generate a broader societal impact. On the other hand, there is a movement among makers that makes 3D printing technology cheap and easy to use. To print an object, computer-aided design (CAD) software is needed (with a price as high as \$50k); however, open-source CAD software is available as an alternative. Also, companies such as Autodesk have made the software affordable. Furthermore, 3D printer makers allow users to upload 3D designs to the cloud, which will help the proliferation of 3D printing.

### From design to 3D objects

3D printing begins with a 3D model using CAD software and converts the model into an STL (surface tessellation language) file. The STL file will be sliced into 2D layers for planning the printing path of 3D objects. However, it is only good for a single color or a single type of material because the file only carries the surface geometry, not the color or texture. An alternative file format, such as OBJ files, can store color, material, and texture information, and PLY files can carry 3D scanned objects. Also, new file formats have been developed, including 3D manufacturing format (3MF) and additive manufacturing format (AMF). Both describe the internal information of 3D models, including color, materials, and texture. Unlike STL, AMF stores geometry data coded in triangular tessellation that can curve, giving accurate geometry. 3MF, an advanced version of AMF, has all the technical properties of AMF, and the data are saved in the human-readable XML format for ease of control.

In terms of materials, polymers are popular in 3D printing due to their design flexibility, ease of use, and cost-effectiveness. Generally, the physical, mechanical, and chemical properties of polymers depend on chemical composition, polymer structures, and the degree of curing. At the material design and synthesis stage, we have the capability to design the inherent material properties at the molecular level,

and then process them into shapes, sizes, and rheology suitable for 3D printing processes. During printing, different manufacturing parameters (e.g., temperature and heating/cooling rate) can influence the material microstructures, such as size and degree of crystallinity, and finally determine the mechanical and other properties of the printed objects. Thus, it is critical to understand the process-structure-property relationships in 3D printing.

For instance, powder bed fusion (PBF) requires spherical thermoplastic powders with a specific range of sizes between 10 and 120  $\mu\text{m}$  for predictable and high-quality parts.<sup>19</sup> Typically, the polymers used for PBF are semi-crystalline with a wide sintering window (temperature range between melting temperature and crystallization temperature).<sup>20</sup> If the sintering window of the polymers is too narrow and the processing temperature is close to crystallization temperature, there will not be sufficient consolidation. Consequently, imperfections can be introduced in the parts, and the printed product might be curled and distorted after release from the surrounding powder bed due to premature crystallization. Another key parameter affecting the polymer structures in PBF is the cooling rate. During cooling (where crystallization occurs), the polymer chains rearrange to form ordered crystalline structures and semi-crystalline regions.<sup>21</sup> If the cooling rate is fast, the crystallinity tends to decrease, affecting the mechanical properties of the printed products.<sup>22</sup> Therefore, in PBF with semi-crystalline polymers, a proper bed temperature (usually 2°C–4°C below the melting peak) and cooling rate should be selected.<sup>23</sup>

In vat photopolymerization (VP), 3D printing is usually accomplished through the UV curing process, which is a photochemical process where UV light is used to initiate the polymerization (or crosslinking network) of resins (typically monomers and oligomers) with the assistance of photoinitiators. The photosensitive polymers (i.e., photopolymer) should be designed to have appropriate viscosity of less than 5 Pa·s for good fluidity and relatively high absorption coefficient, depending on the type of photoinitiators, for high printing resolution.<sup>24</sup> The viscosity of these photopolymers can be adjusted to a lower value by adding reactive diluent or heating the resin during the printing process.<sup>25</sup> Although the reactive diluent is good for viscosity control, the flexible and compressive modulus and ultimate stress gradually decline with the increase of the weight fraction of the diluent.<sup>26</sup> The penetration depth of UV light can be controlled with the addition of a photo-absorber that increases the absorption of the light.<sup>27</sup> The higher absorption of the light leads to higher production of free radicals as the initiator by causing high crosslinking of the polymer chain and degree of curing.

For a successful 3D printing, we first need to understand the materials and choose the right process; then the manufacturing process must be optimized, and finally the quality of the prints should be examined. Post-processing, such as cleaning, surface finishing, curing, and painting, are required in most printing processes. Cleaning includes cutting support material and removing powder. After cleaning the unnecessary parts, surface finishing might be needed to make the product nicer through mechanical (e.g., sanding and bead blasting) and chemical treatments (e.g., vapor reaction). In the case of VP technique, an extra curing process using UV light might be required to enhance the mechanical properties of the printed product. In some cases, the printed object is painted using a brush or spray for visualization.

### 3D PRINTING PROCESS FOR POLYMER AND COMPOSITES

3D printing processes are well established to produce 3D objects composed of polymers and polymer composites. Some 3D printing techniques are well developed,

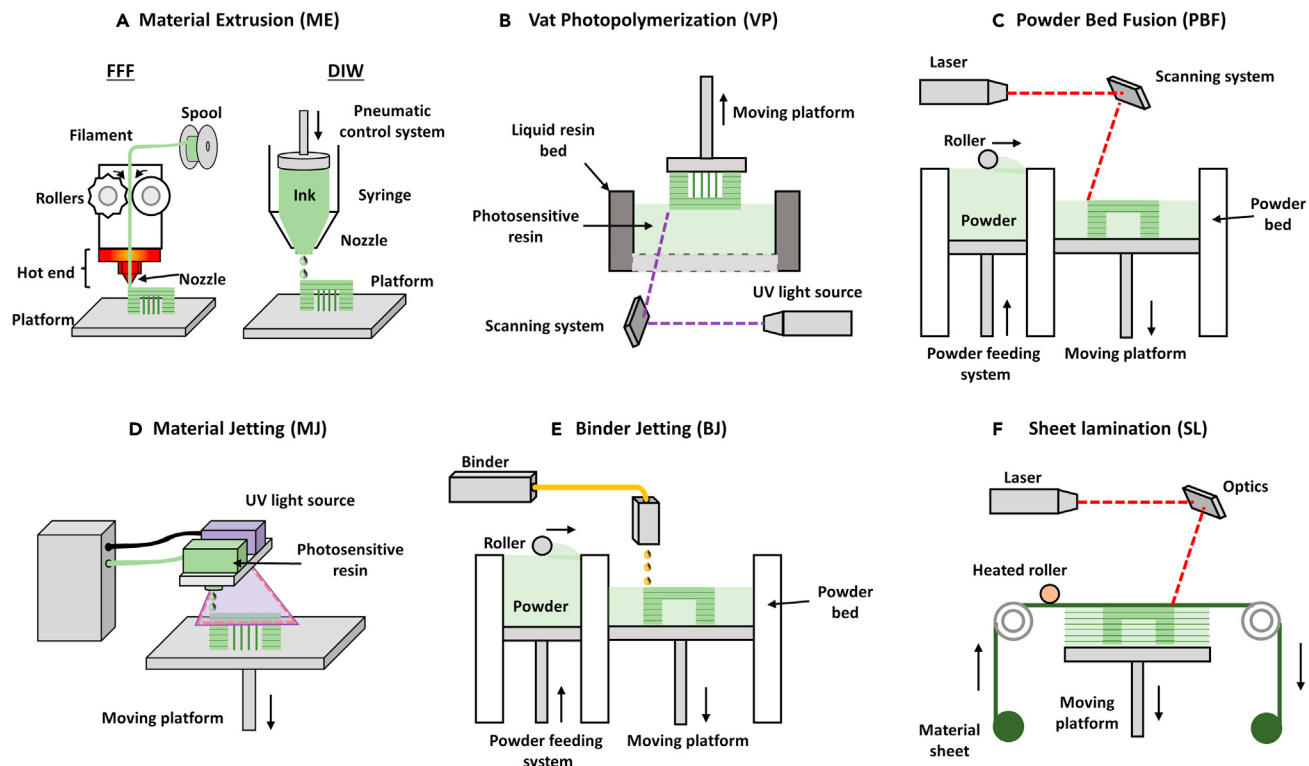


**Figure 2. Schematics of 3D printing techniques**

- (A) In material extrusion (ME), filament fused fabrication (FFF) is a 3D printing method in which the solid filament is melted, extruded through the nozzle, and deposited layer by layer. Direct ink writing (DIW) employs viscoelastic ink, and the ink is extruded through a small nozzle under controlled flow rates.
- (B) Vat photopolymerization (VP) uses UV light to cure the photopolymer resin in the liquid bath by forming crosslinked networks.
- (C) Powder bed fusion (PBF) utilizes thermal energy to melt powdered material and prints out a 3D object.
- (D) Material jetting (MJ) prints out 3D products by selectively depositing the droplets of build materials.
- (E) Binder jetting (BJ) drops liquid binder onto powder materials, which are the main components in final objects.
- (F) Sheet lamination (SL) uses thin sheets of material and bonds together layer by layer to fabricate a 3D object.

such as material extrusion (ME) (we mainly focus on FFF in this review and for direct ink writing we refer to a previous review paper<sup>28</sup>), VP (or stereolithography [SLA]), material jetting (MJ), binder jetting (BJ), and PBF, but many others are still under development.<sup>29</sup> Each 3D printing process has its own advantages and challenges in the fabrication of polymer composites and requires specific conditions of the polymer, such as shape, state (solid or liquid), and physical properties (viscosity and melting temperature). Therefore, when selecting the 3D printing techniques, a user must consider materials, cost, and application requirements (including resolution, the complexity of geometry, and mechanical properties). Herein, we will look at each 3D printing mechanism. Six common 3D printing methods are illustrated in Figure 2, with key components labeled. Their characteristics (printing principle, typical polymers and state of polymers, and advantages and disadvantages) are summarized in Table 1. More details of their characteristics described in Table 1 are discussed separately under each printing mechanism in the following sections “ME,” “VP or SLA,” “PBF,” “Jetting-based processes (MJ and BJ),” and “Sheet lamination.” Also, we also briefly discuss other additive approaches for composites manufacturing.

### ME

ME selectively dispenses a material through a nozzle and deposits the material layer by layer to build a 3D object. ME has a different printing process depending on the

**Table 1.** The characteristics of 3D printing technologies for polymers and composites

	Printing principle	Polymer/composite state	Typical polymer materials	Advantages	Disadvantages
ME (FFF/DIW)	Extrusion	solid filament	thermoplastics, such as polycarbonates, ABS, PLA, and nylon	simple, low cost (\$300 for home use and up to \$2k–\$8k for professional use), and fast (from 50 to 150 mm/h up to 500 mm/h)	nozzle clogging and low quality
	pressurized extrusion	liquid polymer	liquid polymer, hydrogel, and colloidal suspension	material flexibility and high resolution (up to 200 $\mu\text{m}$ )	low throughput
VP	UV-induced curing	liquid photopolymer	photocurable resin (epoxy or acrylate-based resin)	high resolution (6–140 $\mu\text{m}$ )	low throughput (~14 mm/h: ProJet 1200) and high cost (starting around \$3k and up to \$10k for large-volume printing)
PBF	heat-induced sintering	solid powder	polyamide, polystyrene, and PCL powder	good for mass production and design flexibility	high cost (starting at around \$100k), rough surface, and cavity generation
MJ	drop-on-demand material jetting with UV solidification	liquid photopolymer	photocurable resin	high resolution (up to 16 $\mu\text{m}$ ), multi-material capabilities, and homogeneous properties	high cost (\$100k–\$250k: CONNEk3 OBJET350) and not suitable for structural applications
BJ	drop-on-demand binder jetting	liquid polymer	bonding agents + acrylate-based powder (metal and sand)	material and design flexibility and good for mass production	rough surface and cavity generation; shrinkage
SL	layer by layer adhesive	polymer sheet	bonding agents + polymer composites	ease of material handling and fast (45 in <sup>3</sup> /h: CBAM)	varied finish, limited part resolution (50–1,000 mm), and limited mechanical property

material type (liquid or solid). In ME, FFF, also known under the trademarked term fused deposition molding (FDM), is the most commonly used due to its simple setup and cost-effectiveness.<sup>30</sup> FFF is a form of 3D printing wherein the solid filament is melted into the semi-liquid state at the hot end, extruded through the nozzle, and deposited layer by layer on the platform or previously printed layers. Thermoplastic materials, such as polycarbonates, acrylonitrile butadiene styrene (ABS), PLA, and nylon, are used as feedstocks because of their low melting temperature and appropriate viscosity when melted. If composite filaments are employed as feedstocks by adding reinforcements or active fillers, such as carbon nanomaterials, metals, biomaterials, and ceramics, to the polymers, FFF can produce functional products, such as electronics, energy storage devices, and artificial bones. Also, multiple-material (main feedstock and sacrificial feedstock) can be used to manufacture complex structures. The sacrificial materials are used as the support structures, which can be removed completely and leave a good surface finish. The sacrificial feedstocks are usually made of materials dissolvable in a chemical or water, such as polyvinyl alcohol (PVA) and Hydrofill.

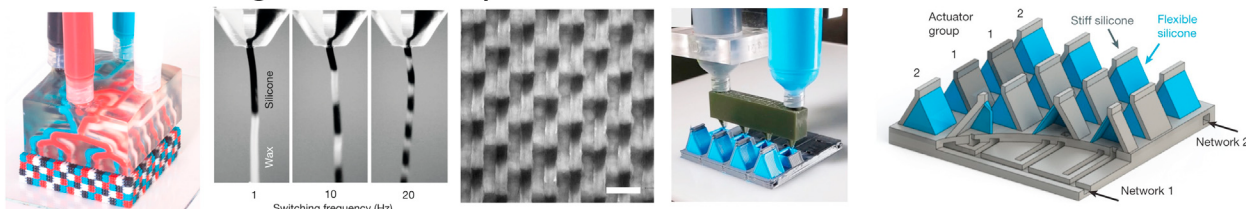
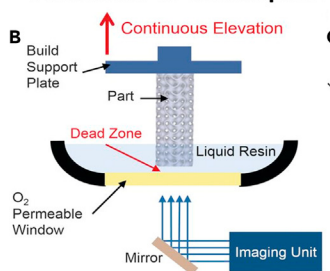
For a successful product printing, it is important to control the feed rate that pushes the molten filament out of the nozzle and keep the compression pressure between the roller and the hot end lower than a critical limit to prevent the filament from buckling.<sup>31</sup> Buckling is one of the most common failure modes in filament extrusion. In 2000, the relationship between buckling and the ratio of the elastic modulus of the filament and the melt viscosity was found experimentally. If the ratio of the modulus of the feedstock and its melt viscosity is above a critical range ( $E/\eta$ :  $3 \times 10^5$  to  $5 \times 10^5 \text{ s}^{-1}$ ), buckling will not

occur.<sup>32</sup> The mechanical properties of the printed objects are affected by the printing speed, temperature, and environmental conditions (temperature and humidity). The generated shear stress in the melted state of a polymer depends on the printing speed and affects the degree of orientation of polymer chains. As a result, the polymer chains tend to be aligned along the printing direction, and the polymer strength along the chain direction is higher than that of the transverse direction. The environment temperature of the 3D printing platform should also be considered because the temperature influences the cooling rate of the melted polymer and the ensuing crystallinity of the re-solidified polymer, thereby affecting the final mechanical performance of the printed object.

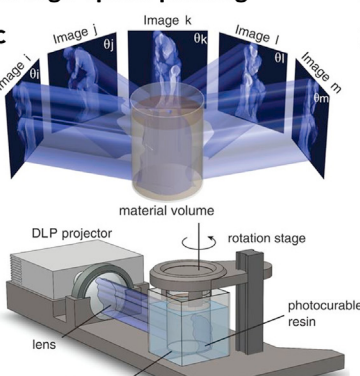
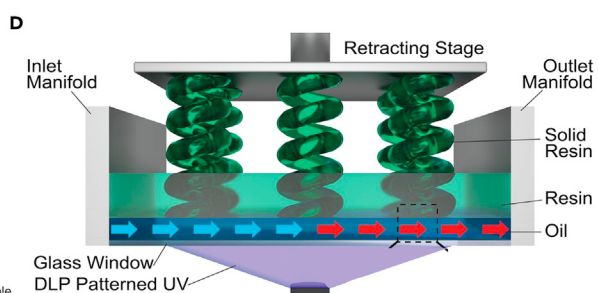
FFF is easily accessible with simple operations and relatively low costs. Desktop 3D printers range from around \$300 for simple use and up to \$2,000–\$8,000 for professional use. Also, in general, this type of machine can quickly produce a 3D object at speeds from 50 to 150 mm/h up to 500 mm/h. In terms of the build size, this is limited by the dimensions of the printing plate and chamber size. FDM printers for domestic purposes can print 3D products with dimensions of 200 × 200 × 200 mm. For industrial purposes, FDM can be enabled to fabricate large objects with dimensions of 1,000 × 1,000 × 1,000 mm. However, this has low resolution compared with other printing techniques, such as VP, due to its nozzle size (usually around 0.4 mm in diameter).

The main issue is that the printed products using FFF have low strength and toughness in the build direction (z axis) due to the weak interlayer bonding and void formation. There are several approaches to alleviate weak bonding and the formation of voids between layers by enhancing the crosslink network between interlayers. One method is to use an optical heating system, such as a laser or infrared (IR) lamp to heat the pre-deposited surface before material deposition, which can enhance the polymer chain diffusion at the interface between the layers.<sup>33</sup> For instance, IR radiation has been used to preheat the surface of the printed area just before depositing the next layer.<sup>34</sup> IR showed effective heating over a wide region above the glass transition temperature, where intermolecular diffusion occurs across the interface, making it suitable for large-area additive manufacturing systems. Another way is by modifying the filament by adding thermal conductive fillers into polymers to help heat generation between interlayers. Filaments coated with carbon nanotube (CNT) were developed to weld the printed interfaces using microwave irradiation.<sup>35</sup> In 2014, the first commercial FFF printer, capable of polymer composite AM, was developed by Markforged. This printer has dual nozzles for polymer and fiber-reinforced filament, working individually. It compresses the printed fiber-reinforced filaments and deforms them from a round shape to a rectangular shape to create a better interlayer bonding. Layer by layer appearance is another issue, especially in FDM, as it has a lower resolution compared with other 3D printing methods, such as PBF or stereolithography. The appearance of the printed products may be important if a flat surface is preferred in applications (e.g., buildings, toys, and aerospace). Therefore, chemical or physical post-processing methods, such as melting, resin casting, acetone finishing, bead blasting, traditional machining, and sanding, will be required for a smooth surface. With FFF, composite products can be fabricated using composite filaments, which are mixtures of reinforcements and polymer matrix. However, the nozzle of the 3D printer may clog easily due to higher viscosity at the melted state, bigger size, or agglomeration of the reinforcements, and the lack of the extrusion forces to push the hard filaments out of the nozzle.

As another type of ME, direct ink wiring (DIW) is an ink-deposition process in which the viscoelastic ink is extruded through a small nozzle under controlled flow rates and

**A Multi-material using voxel-based DIW system****Advanced VP techniques for high-speed printing**

**Example: Continuous liquid interface production (CLIP) and computed axial lithography (CAL)**

**Advanced VP technique for dissipating thermal stress****Example: High-area rapid printing (HARP)**

**Figure 3. Innovation in polymer 3D printing**

(A) Image of multi-material DIW system producing a continuous voxelated filament at increasing switching frequencies and printed soft robots using voxel-based 3D printing. Reproduced with permission from Skylar-Scott et al.<sup>41</sup> Copyright 2019, Springer Nature.

(B) Schematic of the continuous liquid interface production (CLIP) printer in which the oxygen-permeable window creates a dead zone between the printed part and the window. Reproduced with permission from Tumbleston et al.<sup>42</sup> Copyright 2015, American Association for the Advancement of Science.

(C) Schematic of the computed axial lithography (CAL) system using digital light processor (DLP) projector. Reproduced with permission from Kelly et al.<sup>43</sup> Copyright 2019, American Association for the Advancement of Science.

(D) Schematic of a HARP printer where the mobile oil cools down across the entire print area. Reproduced with permission from Walker et al.<sup>44</sup> Copyright 2019, American Association for the Advancement of Science.

deposited layer by layer to create 3D structures. Because of its relatively high resolution (up to 200 µm) and its ability to print meso- and microscale 3D periodic structures, DIW is actively used for functional applications, such as microfluidic devices<sup>36</sup> and sensors.<sup>37</sup> Also, it enjoys material flexibility by adding various fillers in printable ink. For feedstocks, there are polymer liquids,<sup>38</sup> hydrogels,<sup>39</sup> and colloidal suspensions.<sup>40</sup> Direct writing of 3D polymer scaffolds using colloidal gels is generally used. The key point to be considered is material's rheology that ink should behave shear thinning under certain shear stress<sup>28</sup> and relatively good mechanical properties for self-supporting features after dispersing. In most cases, the inks comprise a mixture of powdered materials in liquid polymers, and they are systematically adjusted to achieve sufficient yield stress and shear-thinning behavior through defoaming and cooling or heating.

Recently, a multi-material multi-nozzle DIW system using a high switching frequency was invented to extrude a voxelated multi-material filament.<sup>41</sup> Typically, voxel-based 3D printing uses low-viscosity ink. Multiple viscoelastic materials converge at a junction in the multi-material multi-nozzle 3D (MM3D) printing head, and the 3D printer acts like a diode by using high-frequency switching between up to eight different materials to create voxels with a volume approaching that of the nozzle diameter cubed. Figure 3A shows several printing examples that are multi-material filament and printed soft robots via voxel-based 3D printing.

**VP or SLA**

VP, which is also called SLA, employs photopolymers (epoxy- or acrylic-based resin) solidified by UV light. Top-down VP and bottom-up VP are the main machine setups. In top-down VP, UV light moves in the desired path above the tank and solidifies the photopolymer in the liquid bath on the top by forming crosslinked networks. Once a layer is printed, the platform moves down from the reaction zone by a given layer thickness to allow the fresh, uncured resin to replenish the zone. Then the printer prints the next layer and repeats the processes until the object is complete. Bottom-up VP requires less resin to fill the bath and can make larger volumes compared with top-down VP. The bottom-up VP printers place the light source under the resin bath, and the moving platform is built facing upside down. The resin bath has a transparent bottom that allows the light of the laser to pass through but prevents the cured part from sticking to it. After printing a layer, the cured part moves away from the reaction zone of the bath as the platform moves upward. Also, if the excitation mechanism for polymerization is changed (from single-photon absorption to multiphoton absorption), VP can fabricate 3D objects with high resolution in the sub-micron region.<sup>45</sup> Unlike traditional VP, where polymerization occurs at the surface where the laser irradiates, two-photon polymerization (TPP) cures only in a tightly focused spot (usually inside the photopolymer). In TPP, the photochemical process is induced by a femtosecond laser beam, and the resin molecule absorbs two photons simultaneously to activate the polymerization.

Photopolymers typically consist of monomer/oligomer and photoinitiators, but for a proper photo-initiation process and high-quality products, diluent and chain transfer agents can be added.<sup>46</sup> Diluent agents control the viscosity of the resin for proper wetting and impregnating, and chain transfer agents modify the crosslink network during printing. For a good polymer curing process, several curing reaction factors, including the intensity of the laser, viscosity, and wetting behavior of the resin, should be well controlled.<sup>46,47</sup> As the vat limits the presence of multiple photopolymers in an unmixed state, it is challenging to print multi-materials with this technology unless multiple reservoirs are used for different photopolymers or integrated with a microfluidic system to actively exchange different photopolymers.<sup>48</sup>

The high resolution of VP (around 6–140 μm) is helpful to manufacture precise objects in the range of hundreds of micrometers, but it is time-consuming to fabricate large samples due to low printing speed (~14 mm/h in the vertical direction; ProJet 1200).<sup>45</sup> Also, the printer is more expensive compared with a FFF printer, starting at around \$3k and up to \$10k for large-volume printing. In the case of VP, post-processing (washing and curing) may be required. Normally, isopropyl alcohol or tripropylene glycol monomethyl ether is used to clean the surface, which removes the sticky and excess resin on the printed object. In some cases, post-curing is needed to improve mechanical properties using UV light and heating. It is noteworthy that, during VP, the generated thermal stress can deform the structure, which should be seriously considered especially if exploring high-speed printing. One of the advanced VP techniques is continuous liquid interface production.<sup>42</sup> This addresses the low printing speed by using an oxygen-permeable window to generate a persistent liquid interface where photopolymerization is inhibited, as illustrated in [Figure 3B](#). Another advanced VP for high printing speed is computed axial lithography (CAL), which illuminates a rotating volume of photosensitive resin with a dynamically evolving light pattern.<sup>43</sup> As shown in [Figure 3C](#), the CAL system uses a digital video projector to deliver light energy as a set of 2D images, and the resin exposed to the light from multiple angles solidifies in the desired 3D geometry. [Figure 3D](#) shows an advanced technique designed to mitigate the generated thermal stress, called

high-area rapid printing. This uses mobile oil to dissipate the heat and reduce adhesive forces as well as allowing for a continuous and rapid printing process.<sup>44</sup>

As an alternate method for alleviating the limited mechanical property of brittleness caused by the many crosslinks and stiff backbone of the photopolymers, diverse fillers, such as inorganic compounds, are used by premixing them with the resin.<sup>49</sup> However, the reinforcements can induce high viscosity, low photosensitivity, and inhomogeneity, which makes high-quality printing challenging.

### PBF

PBF is one of the most versatile technologies, which is already popular in mass production. It uses powder material and prints out 3D shapes by selectively injecting thermo-energy, such as lasers. The laser passes over the surface of the powders, sintering them selectively and fusing the powder together to form the desired shape for each 2D layer. During printing, the temperature of the powder bed is slightly below the melting temperature to minimize the heat needed to melt the powder but above the crystallization temperature to retard crystallization. After printing one layer, a roller brings additional powders from the supply platform, recoats the printed layer, and then repeats the operations. Although theoretically any thermoplastic polymer powder can be used as a feedstock, polyamide and polycaprolactone (PCL) powders are primary materials in practice, as they feature a wide sintering window<sup>50</sup> and consolidation behavior.<sup>51</sup> In PBF, major printing parameters include powder size, laser power, layer thickness, and scanning speed. These parameters should be considered for a proper powder recoating step, appropriate mobility of the melted powder, and low porous and high geometric accuracy, respectively.<sup>52</sup>

PBF enables the manufacturing of many products at the same time and can print complex objects because the powders act as supports. The size of a product depends on the volume of the PBF machine, and the resolution of the printed layer is relatively high (~60 µm; EOS P 396). The printed feature size is related to the beam diameter and powder size. The build volume of the machine is relatively large but limited by the chamber size (340 × 340 × 600 mm, which is in the medium build volume range; EOS P 396). However, the cost of a printer is high, starting at around \$100k, and the printed products have a rough surface and require post-processing to smooth the surface through methods such as chemical (using chemical vapors), mechanical (sanding and bead blasting), and laser polishing. In addition, limited reinforcements can be used for the fabrication of composites since only discontinuous reinforcements are compatible with PBF powder feeding.

### Jetting-based processes (MJ and BJ)

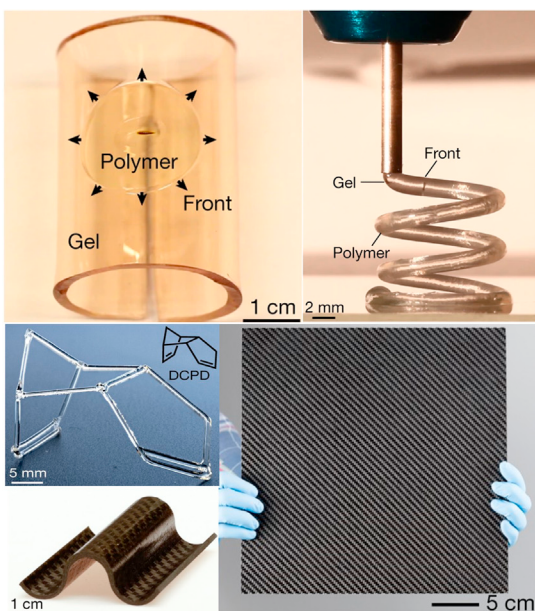
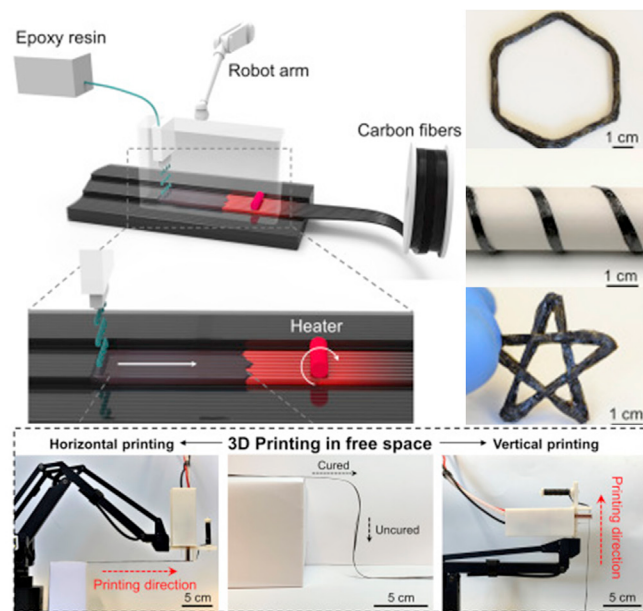
In the jetting-based processes, MJ and BJ are typical types of 3D printing. MJ was introduced for producing a full-color visual prototype in the 1990s. MJ manufactures 3D products by selectively depositing the droplets of build materials. It is one of the most accurate printing technologies (up to 16 µm) and can print multi-material products using multiple nozzles.<sup>53</sup> It generally offers high-quality prints with a smooth surface finish at an efficient printing rate (normally 2,800–4,000 cm<sup>3</sup>/h [Jet Fusion 3D 4200] and 4,500 cm<sup>3</sup>/h for a high-performance printer [HP Jet Fusion 3D 4200]), but the equipment costs around \$100k–\$250k (CONNEX3 OBJET350). The liquid state resins (usually photopolymers) are dropped on desired positions and cured by UV light that is located near the printing head. Once each layer is completed, the build platform moves down or the printing head moves up, and the process repeats until the whole part is printed. Similar to other 3D printing methods, it is common to conduct post-processing, such as support removal, surface finish, and dying.

In MJ, the rheology (viscosity and shear thinning) of the liquid resin is the main parameter.<sup>54</sup> The polymer should have a shear-thinning behavior to fluidize and flow through the small nozzle and then rapidly recover its modulus after exiting the nozzle to maintain the printed structure. In addition, the liquid polymer must have a suitable viscosity to drop on demand. For this reason, the photopolymers are pre-heated up to 30°C–60°C. The limited viscosity in the range of 20–40 centipoise is the most problematic point for droplet formation, making it difficult to design printable materials.<sup>55</sup> In addition, other factors, including liquid density and surface tension, need to be finetuned to successfully convert a printing material from a continuous liquid into small droplets. The mechanical properties of printed objects are not suitable for structural prototypes due to the brittleness attributed to the formation of polymer networks with high crosslink density,<sup>25</sup> but they can be enhanced by adding nano-fillers (silica and clay) in ink. However, these nano-fillers are discontinuous, and the enhancement in mechanical properties is not sufficient for structural applications.

The BJ process drops liquid binder onto a powder bed, which will become the main components in the final objects. The printing steps are almost the same as PBF discussed above, except for the curing process, as solvent welding or chemical reaction occurs between the powder and the binder without thermal processing. This non-thermal process widens the range of the materials compared with PBF: the final products can be made of many different materials as long as they are supplied as a powder, and the binder can be varied depending on the powder used. Similar to PBF, it is effective for mass production and allows the production of high-resolution products (~35 µm), but the final products have lots of pores inside the structure after removing the binder, which requires additional post-treatment to infill materials inside porous structures for mechanical property enhancements. In general, a line is installed to inject materials into the pores inside the products during furnace processing. Moreover, the surface of the product is rough and requires post-processing to smooth the surface. In BJ, powder size, binder viscosity, printing speed, and wetting the powder with the liquid binder should be controlled for high-quality products.<sup>56</sup>

### **Sheet lamination**

As one of the typical additive manufacturing methods, sheet lamination (SL) can also be used for polymer composites AM by bonding sheets of materials to form a 3D part. Polymer composites can be printed by laminated object manufacturing technology, which uses thin sheets of material and adhesive instead of welding. In this printing process, heat and pressure are used together to melt and bond the sheets together. When layer by layer bonding is complete, the unnecessary area is trimmed in the current piece of material to form a designed layer for the 3D object. Material handling is easy in SL, making it suitable for rapid production. However, the resolution (normally 50–1,000 mm in the z-direction) is limited due to the fixed sheet thickness, and the mechanical properties are determined by the adhesive strength. In addition, it may require post-processing to polish the surface and heat treatment to enhance the interlayer bonding. One of the successful companies, Impossible Objects, has successfully printed 3D objects in SL using composite materials (e.g., carbon fiber sheet and glass fiber sheet). This SL process applies adhesive on the sheets, dispenses polymer powder on each sheet, and then bonds the sheets. The printed object is heated in an oven to melt the polymer and compressed to consolidate the part. After that, excess material is trimmed away through a mechanical or chemical process. The printer can build a structure with the maximum volume of 12 × 12 × 4 inches at high speed (45 in<sup>3</sup>/h: CBAM).

**A Polymer innovation for composite****Example: Frontal polymerization****B 3D printing technique innovation for composite****Example: Localized in-plane thermal assisted (LITA) 3D printing****Figure 4. Innovation in fiber/polymer composite 3D printing**

(A) Free-form 3D-printed thermoset structures and carbon fiber-reinforced polymer composite parts produced by the frontal ring-opening metathesis polymerization. Reproduced with permission from Robertson et al.<sup>57</sup> Copyright 2018, Springer Nature.

(B) Schematic of localized in-plane thermal-assisted 3D printing using dynamic capillary-driven infusion and curing of thermosets and 3D printed samples on a cylindrical rod and in free space. Reproduced with permission from Shi et al.<sup>58</sup> Copyright 2020, Elsevier B.V.

**Advanced 3D printing technologies using thermal-curable thermosets**

Thermal-curable thermosets have excellent mechanical properties and thermal stability, but their viscosities significantly decrease during curing. Thus, they are not widely used in 3D printing. To overcome this limitation, two representative approaches are discussed in this section, one is through polymer design, and the other is through 3D printing technology innovation.

In the first approach, thermosetting polymers are designed to provide the energy for materials synthesis using the enthalpy of polymerization rather than using an external energy source. The well-controlled polymer curing strategy was called frontal ring-opening metathesis polymerization (FROMP), in which a solution of a monomer (e.g., dicyclopentadiene) and an initiator (e.g., ruthenium) is heated locally until the initiator is initiated to polymerize the monomer, and the produced heat from the polymerization drives the further reaction.<sup>57</sup> As shown in Figure 4A, the gel cured by FROMP can be applied not only to 3D printing for producing free-standing thermoset structures but also to the fabrication of carbon fiber-reinforced polymer composite parts, which can be cured within 5 min.

In the second approach, a new concept of 3D printing is developed by leveraging a thermal-induced dynamic capillary to print carbon fiber-reinforced thermoset composites, called localized in-plane thermal-assisted (LITA) 3D printing.<sup>58</sup> LITA 3D printing enables near-simultaneous infusion and curing of the composites based on a continuous capillary effect driven by a moving thermal gradient along with

the carbon fiber. During printing, the liquid polymer flows into the space between the carbon fibers, then is cured quickly from the heated fiber surfaces to the surrounding space. [Figure 4B](#) shows a wide range of printing abilities, such as printing the complex shapes of composites, printing on curved surfaces, and printing in free space.

## MATERIALS DISCOVERY FOR AM TECHNOLOGIES

### Polymer design and selection for AM of polymer composite

AM technologies have specific material property requirements, such as melting point, and rheology properties. Thermoset polymers and composites are essential for lightweight, energy-efficient structures in the aerospace, automotive, and energy industries. However, the fabrication of high-performance thermosets, except for the photocurable resins, needs high temperatures (around 180°C) to cure the monomers for several hours. Thus, these thermosets are difficult to be used as feedstocks for 3D printing. By designing the polymer, especially polymerization kinetics, rapid curing of the polymer at the ambient temperature has become possible, and it has provided an opportunity to expand material choices in 3D printing.<sup>57</sup> Therefore, it is critical to design and select polymers for AM based on a fundamental understanding of polymer characteristics.

Two widely used 3D printable polymers are thermoplastics and UV-curable thermosets (i.e., photopolymers). Another special class of polymer is hydrogel, which has a network of hydrophilic polymer chains. These three kinds of polymers are popular in 3D printing, and their molecular structure, critical physical properties, sub-categories (such as representative polymers), and common printing methods are shown in [Figure 5](#).

#### *Thermoplastic polymers*

Thermoplastic polymers are commonly used polymers that soften when heated, allowing for shaping, and solidify again when they cool down. Thermoplastic polymers can be divided into amorphous and semi-crystalline plastics based on their molecular structure illustrated in [Figure 5A](#). Amorphous thermoplastics have a randomly ordered molecular structure that lacks a sharp melting point, making them easy for thermoforming. On the other hand, semi-crystalline thermoplastics have a highly ordered molecular structure with a sharp melting point. After a certain quantity of heat is absorbed, they suddenly become liquid from a solid state. The semi-crystalline polymers have good mechanical properties due to their strong intermolecular forces. All thermoplastic polymers have reversible processing capability, making them suitable for extrusion-based 3D printing, such as FFF. Under external heat from a 3D printer, solid polymer particles (or filaments) are melted by breaking the polymer chains. At this stage, polymer chains can move freely and, after printing, the melted polymer is solidified in the desired arrangement, and the polymer chains become interconnected and immovable again.

Feedstock thermoplastic polymers, including ABS, PLA, polyamide-nylon, and polyethylene terephthalate glycol, are commonly used as filament for FDM. The low melting temperature and proper mechanical properties of these standard polymers make them popular as 3D printing materials. But these standard thermoplastics cannot be used in applications requiring high mechanical properties and chemical/thermal stability. To remedy this, researchers have developed extrusion printers for high-performance thermoplastics,<sup>27</sup> such as polyether-ether-ketone and polyethyleneimine, which require higher processing temperatures. Most high-performance polymers have a special single mechanical or thermal property, but generally

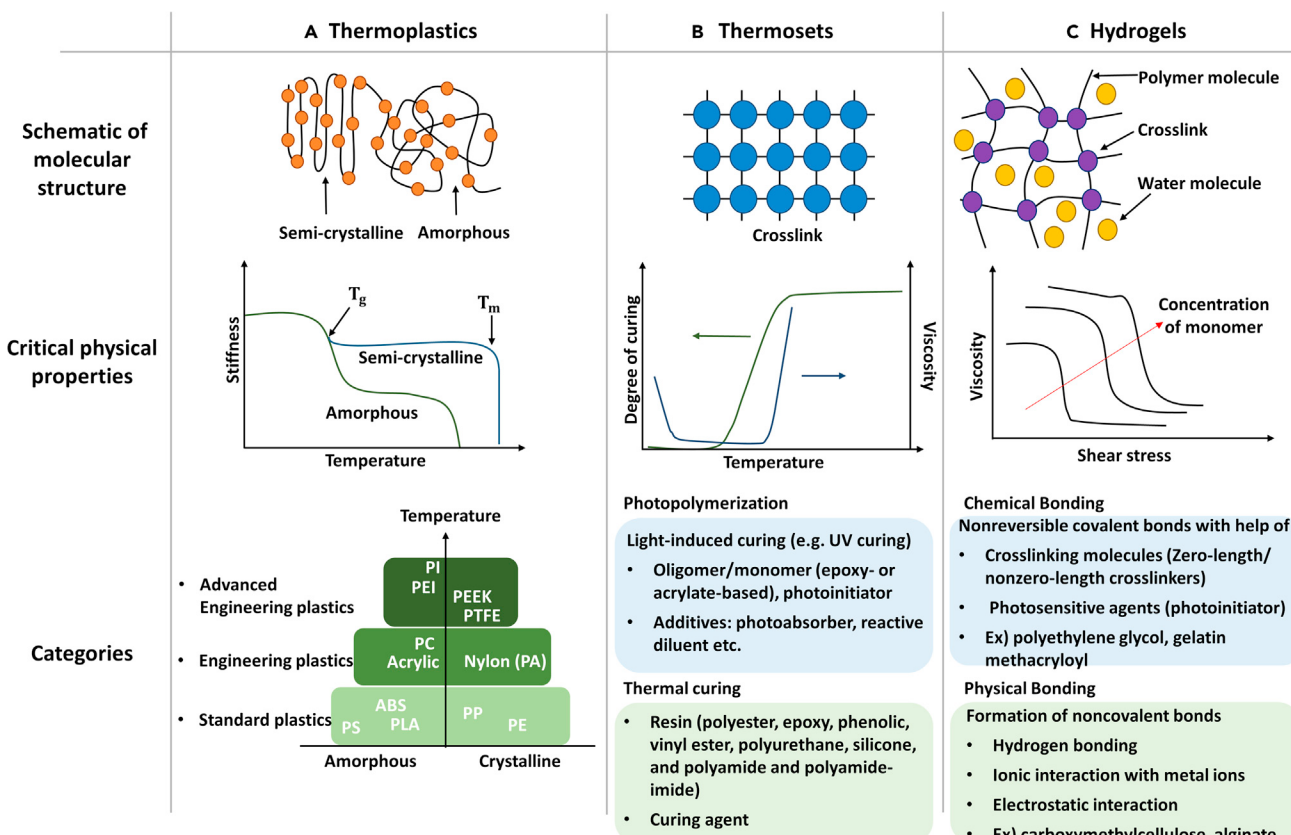


**Figure 5. Commonly used polymers in 3D printing and their properties**

(A) Thermoplastics, (B) thermosets, and (C) hydrogels.

they have a high level of physical properties and good resistance to degradation. Table 2 summarizes the physical (glass transition and melting temperature) and mechanical (elastic modulus) properties of thermoplastic polymers widely used in extrusion-based 3D printing. This table can be used as a reference for selection of materials and new polymer development. It is envisioned that 3D printable polymers with high melting point and high mechanical performance will play an important role in structural applications.

### Thermosets

Thermosetting polymers are irreversibly hardened by curing a viscous liquid prepolymer or resin. Rather than just growing in one direction, the active reaction sites inside the polymer chain react with their adjacent chains to form a tightly connected polymer network. The higher the crosslinking density of the thermosets, the higher mechanical strength and hardness, and the higher the resistance to heat degradation and chemical attack. These polymers can be cured by heat or suitable radiation and be promoted by high pressure and the addition of catalysts. Figure 5B shows the connected molecular structure of thermosetting and describes various components depending on the curing methods. In the case of thermo-curing polymers, the curing reaction becomes active as the temperature increases, but the reaction becomes slow when the system reaches the glass transition and continues until the complete curing of the resin. By contrast, photopolymers are initiated with UV radiation, which is more energetic. UV light triggers the break of a covalent bond or ionic bond of photoinitiators and generates the active free radicals or active cationic/anion groups

**Table 2. Physical and mechanical properties of thermoplastics widely used in extrusion-based 3D printing**

	Glass transition temperature (°C)	Melting temperature (°C)	Modulus (GPa)
ABS	102–115	–	1.8–2.39
PLA	53–64	145–186	1.2–3.0
Nylon 6	47–57	220	2.8–3.1
Polyethylene terephthalate glycol	75–80	–	0.9–1.1
Polyether-ether-ketone	137–152	335–343	3.56

for the rapid polymerization of the monomers in photopolymer resins. Once it is initiated, the chain reaction will develop as in a conventional thermal polymerization, except for the initiation stage, in which the rate of initiation can be increased by high irradiation.<sup>59</sup> Among various photopolymers, acrylate-based polymers, including acrylate polyesters, and acrylate silicone, and acrylate urethanes, have been actively used because the polymerization rate of their radical chain reaction is very fast.

Photopolymer resins (epoxy- or acrylate-based) are primarily used in VP and droplet-based 3D printing (such as inkjet printing). They typically polymerize under UV light with a wavelength between 355 and 405 nm. In this approach, low viscosity or good fluidity of the photopolymer is necessary. The photopolymers with low viscosity are composed of small-molecular-weight monomer and oligomers. Such photopolymers are easy to be cured with a high crosslinking degree, resulting in hard and brittle structures. If the resin is composed of high-molecular-weight compositions, the viscosity will be high. To deal with high viscosity, reactive diluents are added into the resin, but they can become part of the final structure of the polymers and potentially deteriorate the performance of prints.<sup>59</sup> Ideally, the development of photopolymer resin should meet two criteria: low viscosity and high performance.

### Hydrogels

Hydrogels are attractive materials for 3D printing since they are one of the most feasible ink materials for extrusion-based 3D printing.<sup>60</sup> The hydrogel has a 3D crosslinked hydrophilic polymer network (shown in Figure 5C), and it can be classified depending on the preparation methods as a homopolymer, copolymer, and semi-interpenetrating network (semi-IPN).<sup>61</sup> Homopolymers are composed of one type of monomers, such as poly(hydroxyl ethyl methacrylate) (PHEMA) and polyethylene glycol (PEG). Copolymers contain two types of monomers: for example, PEG-PEGMA and carboxymethyl cellulose. Semi-IPN, for example, acrylamide/acrylic acid copolymer, is formed when a linear polymer penetrates another crosslinked network without any chemical bonding between them. Typical solvents, such as water, ethanol, water-ethanol mixtures, and benzyl alcohol, are used for solution polymerization.<sup>62</sup>

High elasticity and softness make hydrogels prominent in bioengineering, smart devices, and agriculture fields.<sup>63</sup> 3D printing is actively adopted for creating small-scale 3D porous scaffolds, such as artificial bone, but it might be difficult to fabricate large and complicated products due to the weak structural stability and large swellability. To be 3D printed successfully, hydrogels should have appropriate rheological properties (viscosity and shear thinning) for printing and strong mechanical integrity to maintain the structure during and after printing. The viscosity of the hydrogel is decided by the monomer concentration and chain length of macromolecules in Figure 2C.<sup>64</sup> The higher monomer concentration and longer chain length

of macromolecules make extended contact between them and lead to enhanced intermolecular attractions, resulting in higher viscosity. The shear-thinning behavior of the hydrogel is possible through a self-assembly process.<sup>65</sup> The self-assembly process can be achieved due to a balance between the forces for assembly (e.g., hydrogen bonding and ionic interaction, and electrostatic interaction) and forces against assembly (e.g., electrostatic solvation). These interactions formed by noncovalent bonding are generally weak but can form stable network structures of the hydrogel. The dynamic structure of these networks dissociates under the applied shear stress and reassembles the network after removing the force to enable self-assembly, leading to shear-thinning behavior. The swelling and mechanical properties of the hydrogel are closely related to the crosslinking density (lower crosslinking density leads to high swellability and low mechanical performance). Depending on the nature of the polymeric backbone and their functional groups, hydrogels could be crosslinked via the chemical and physical methods.<sup>66</sup> Chemical crosslinking takes place with a form of nonreversible covalent bonding between polymeric chains. The chemical network formation occurs by adding chemical crosslinkers (zero-length and nonzero-length crosslinkers) or through chemical reactions, such as enzymatic crosslinking and UV light. Zero-length crosslinkers, such as 1-ethyl-3-(3-dimethyl aminopropyl) carbodiimide, do not affect the final structure of the hydrogel; on the other hand, nonzero-length crosslinkers (e.g., sodium bicarbonate<sup>67</sup> and formaldehyde<sup>68</sup>) become part of the final structure of the hydrogel. Physical crosslinking is a form of noncovalent bonding, such as hydrogen bonding, ionic interaction using metal ions, and electrostatic or hydrophobic interaction. These hydrogels cross-linked by physical crosslinking are generally mechanically weaker than those cross-linked by chemical crosslinking.

### Filling materials

The 3D printed polymer products can have complex geometries, but they are often not ideal for functional applications due to their insufficient or lack of mechanical properties and functionality. Therefore, various filling materials are used to give polymers the desired mechanical, electrical, and other functions. Filling materials can range from the nanoscale (e.g., CNT, graphene, and nanoparticle) to the macro-scale, including chopped or long fiber (e.g., carbon fibers and glass fibers) and woven fabric. For structural enhancement, fibers with high stiffness and strength are widely used as reinforcement materials. Fibers, such as glass fibers, carbon fibers, and aramid fibers within polymer composites, withstand most applied force and act like crack bridging when the composites break, resulting in high stiffness and strength of the composites. In functional applications, including energy storage (e.g., battery and supercapacitor) and electronics (e.g., sensor, electrical circuit, and robot), most classes of materials, including ceramic,<sup>69,70</sup> metal/metal oxide,<sup>71</sup> living cells,<sup>72</sup> can be used. They introduce functionalities, including electrical and thermal conductivity, magnetic properties, and optical properties in polymer composites. Table 3 summarizes the various fillers used in polymer composites for different applications.

### SMART POLYMERS AND 4D PRINTING (SHAPE-MORPHING SYSTEM)

In recent years, the interest in new materials that can provide the desired response under external stimuli has been increasing for the development of active devices, sensors, and actuators in various advanced applications, including biomedical and electronic fields. One class of novel materials is smart materials, which can change their properties, such as shape, color, or size, in response to external stimuli, such as light,<sup>8,12</sup> heat,<sup>6,7,14</sup> humidity,<sup>81</sup> or electric<sup>13</sup> and magnetic fields.<sup>9</sup> Such

**Table 3. Summarization of filler innovations of polymer composite for different applications**

Functionality or application	0D (nanoparticles)	1D (nanofiber and nanowires)	2D (atomically thin sheets)	Others
Electrical application	metal NPs <sup>71</sup> (Au, Ag, Cu, etc.); metal oxides (ZnO, SnO)	CNT, <sup>73</sup> Ag NW, carbon nanofiber (CNF)	graphene <sup>74</sup>	liquid metal, <sup>75</sup> living cells, <sup>72</sup> bacteria, <sup>76</sup> etc.
Biocompatible application	mineral (nano-hydroxyapatite <sup>77</sup> )	fibrin <sup>78</sup>	N/A	
Actuator	ZnO, PZT NPs, <sup>9</sup> magnetic NPs <sup>9</sup>	ZnO NWs	MXene <sup>79</sup>	
Mechanical application	ceramic NPs, <sup>69,70</sup> TiO <sub>2</sub>	CNT, CNF	graphene	
Thermal application	Bi <sub>0.5</sub> Sb <sub>1.5</sub> Te <sub>3</sub> (BST), <sup>80</sup> Ag	CNT, <sup>35</sup> Ag NWs	graphene, BN	

programmable materials add a fourth dimension to 3D printing (i.e., 4D printing), enabling 3D printed objects to transform over time. 4D printing uses the same process as 3D printing, but the printed objects can alter their shape or properties over time in response to external stimuli.<sup>82</sup> This means that 4D printing focuses more on the material system for the desired dynamic structures and applications. Among various 3D printing technologies, FFF, DIW, VP, and SL are actively utilized for 4D printing. FFF can easily fabricate 3D shape-changing objects by leveraging the difference in coefficients of thermal expansion (CTE) between materials. As one of the smart materials, hydrogels are widely used in DIW, and the anisotropic swelling behavior of the printed material (determined by the printing direction) can be leveraged to morph to a desired shape. VP has been actively applied to 4D printing because it can utilize a variety of smart materials by adding smart polymer molecules to the resin and can produce 3D objects with different mechanical properties by controlling light. The anisotropy of the mechanical properties of the products can be used as a principle for shape changing under external stimuli.

Many smart polymers, such as SMPs, smart hydrogel, and LCPs and LCEs, have already been developed, but these materials have limitations. For example, some smart polymers react with a minimal response for a long time or have limited reversibility of the transformation. Even though 4D printed objects require more development for quick and accurate transformation, 4D printing offers new opportunities in diverse applications, including textiles,<sup>83</sup> aerospace,<sup>84</sup> medical industries,<sup>85</sup> electronics,<sup>86,87</sup> and robotics.<sup>88</sup> In this section, we cover smart polymers for 4D printing, especially SMPs, smart hydrogels, and liquid crystals.

### SMPs

SMPs are polymeric smart materials that can return from a deformed shape to the original shape under an external stimulus, such as temperature,<sup>6,7</sup> light,<sup>8</sup> and magnetic field.<sup>9</sup> Through the programming process, including shape deforming, shape fixing, and evacuation of the external stress, the polymer transforming pathway can be controlled, and multiple shape memory effects are also available so that the polymer transitions into a set of shapes. Because of these unique features, SMPs are prominent in various areas, such as smart fabrics,<sup>83</sup> heat-shrinkable tubes for electronics or films for packaging,<sup>86</sup> self-deployable sun sails in spacecraft,<sup>84</sup> and medical devices.<sup>85</sup> The advent of 4D printing, which combines 3D printing technologies and SMPs, enables the design and fabrication of dynamic structures essential for the manufacture of custom products.

One common external stimulus is thermal triggering. The SMP is deformed at a temperature higher than the transition temperature, cooled below the transition

temperature, and fixed in a deformed form. When heating the SMPs above the transition temperature, they recover their original shape due to entropic elasticity. Thermal energy can be applied directly to the structure, but when additional functional materials (e.g., carbon nanotube<sup>73</sup> and magnetite<sup>9</sup>) are added, the structure can be actuated remotely. One example is the shape-changing structure under the magnetic field, as shown in [Figure 6A](#), where the structure made of poly(lactic acid) and magnetic iron oxide ( $\text{Fe}_3\text{O}_4$ ) nanoparticles can be heated remotely under magnetic fields through hysteresis.<sup>9</sup> The shape-changing structures are produced by DIW printing with UV curing. The transforming mechanisms are the same as other examples using thermal response, but the structure has fast, remotely actuated behaviors and magnetically guidable properties.

Another method to activate SMPs uses a heat-shrinkable property. This strategy does not require a shape-programming step. [Figure 6B](#) shows a 3D configuration that transforms from a planar sheet into the final flower structure under temperature change.<sup>6</sup> The release of internal strain in the polymer, generated during the FDM, keeps the printed composite flat under heating. When cooled to room temperature, the printed structure transforms into a flower structure due to the mismatching CTE between different materials. [Figure 6C](#) illustrates another example using time-lapse to show the evolution of shape with temperature change.<sup>7</sup> In this example, both geometry and printing patterns, such as dimensions, the number of grooves, and active elements were controlled during printing to make the floral leaves transform their shape at different times.

### Smart hydrogel composites

Hydrogel composites have great potential as smart materials due to their swellable behavior upon water immersion while maintaining the structure. They have interesting applications varying from biomedical fields (drug delivery devices<sup>89</sup> and artificial organs and tissue engineering<sup>90</sup>) to agriculture.<sup>91</sup> 4D printing for these smart hydrogel composites offers an innovative, versatile, and convenient method for many fields, including custom-designed sensors<sup>87</sup> and robotics.<sup>88</sup> For instance, [Figure 6D](#) describes functional folding flowers made of biomimetic hydrogel composites, which can be folded and twisted.<sup>3</sup> The main principle of shape transformation is the anisotropic swelling behavior of the hydrogel composite controlled by the alignment of cellulose fibrils along with printing directions. Another way to make various responses in one hydrogel structure is to use different components with different swelling properties. As shown in [Figure 6E](#), sea stars are one example of actuating through spatially controlled swelling produced by VP.<sup>10</sup> The sea stars consist of a stiff center region and multicomponent arms. The center section is comprised of a strain-limiting area (purple color) manufactured via UV irradiation, and the arms contain more swellable materials (white color) printed by visible light irradiation. These different swelling behaviors of components make them gradually curl toward the center regions over time in the water, as shown in [Figure 6E](#). [Figure 6F](#) gives the final example: left-evolving bars composed of bars, links, and disks.<sup>11</sup> The bars, disks, and bottom parts of the links are made of a rigid material (marked as white), and hydrogel at the top of the links (marked as red) enables the folding of the structure.

### LCPs and LCEs

LCPs are unique thermoplastics that exhibit properties between highly ordered crystalline solids and are amorphous over a temperature range. LCEs are slightly cross-linked liquid crystalline polymers that can transfer between a highly ordered crystal state and an isotropic amorphous state under external stimuli, such as light,<sup>12</sup>

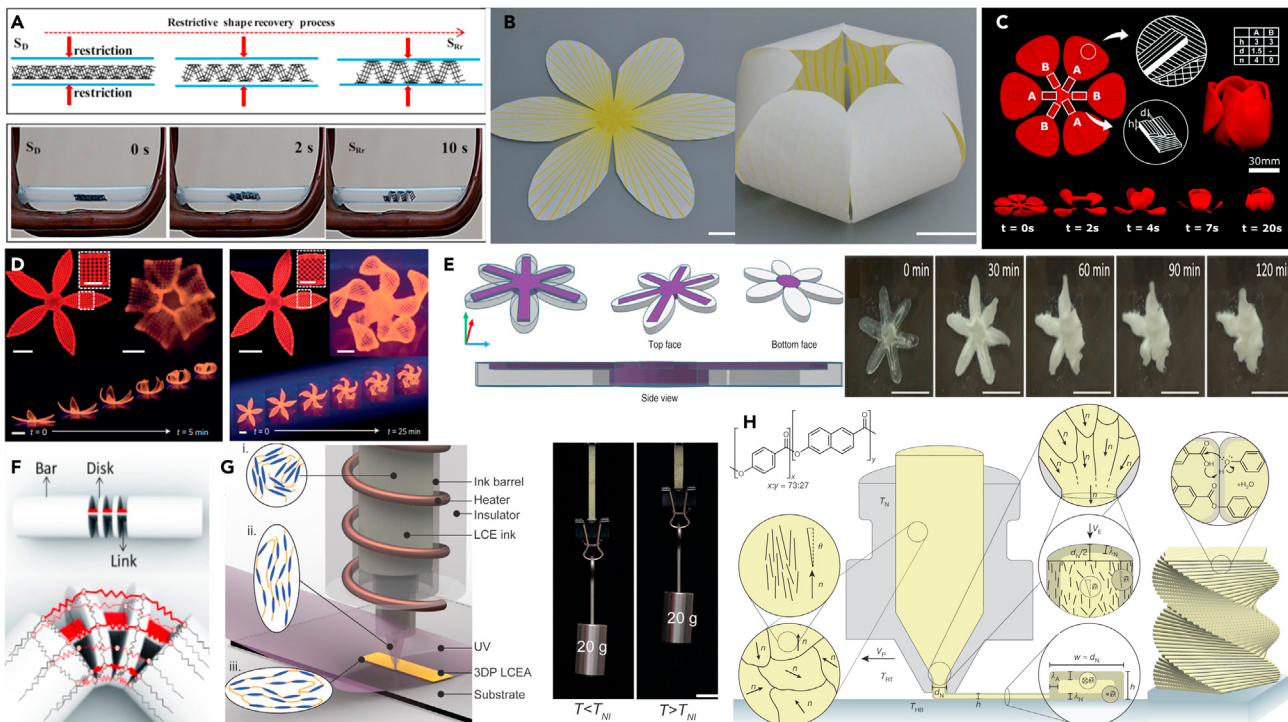


**Figure 6. Polymers composites for 4D printing**

(A) Schematic and demonstration of the restrictive shape recovery process triggered by an alternating magnetic field. Reproduced with permission from Wei et al.<sup>9</sup> Copyright 2016, American Chemical Society.

(B) Flower-like 4D structure from the original flat sheet to the final flower structure. Reproduced with permission from Zhang et al.<sup>6</sup> Copyright 2016, Springer Nature.

(C) The time-lapse illustration to show the sequence of folding of tulip. Reproduced with permission from Van Manen et al.<sup>7</sup> Copyright 2017, Royal Society of Chemistry.

(D) 4D printed flower morphologies with different bilayer direction ( $90^\circ/0^\circ$  and  $-45^\circ/45^\circ$ ). Reproduced with permission from Gladman et al.<sup>3</sup> Copyright 2016, Springer Nature.

(E) CAD models of multi-material sea stars and demonstration of swelling of the sea star in water over time. Reproduced with permission from Schwartz and Boydston.<sup>10</sup> Copyright 2019, Springer Nature.

(F) Illustration of an initial joint and folding of bars with spring-mass systems. The black springs are the rigid bars and disks, and the red springs are the links that can be folded. Reproduced with permission from Raviv et al.<sup>11</sup> Copyright 2014, Springer Nature.

(G) Schematic of the LCE ink during hot-DIW; disordered LCE ink in the barrel (i), aligned LCE ink within the nozzle (ii), and crosslinked LCE filaments after printing (iii), and the image of the printed LCE actuator with meander-line print path, which shows different elongation states depending on the temperature; higher or lower than the nematic-isotropic temperature ( $T_{NI}$ ). Reproduced with permission from Kotikian et al.<sup>14</sup> Copyright 2018, Wiley-VCH Verlag GmbH & Co.

(H) Schematic of printing a core-shell microstructure with a highly aligned shell using FFF. Reproduced with permission from Gantenbein et al.<sup>15</sup> Copyright 2018, Springer Nature.

electricity,<sup>13</sup> and temperature.<sup>14</sup> Due to its unique properties, LCE stands out as a material for soft actuators, artificial muscles, soft robots, and active structures. One example is LCE actuators (LCEAs) with spatially programmed nematic order using high operating temperature DIW.<sup>14</sup> The drawing force generated by the extrusion printing process causes the mesogen units to align along the printing direction, and the alignment of the mesogen facilitates reversible and repeatable contraction in the parallel direction of the aligned mesogen. Figure 6G shows the changes in morphologies of photopolymerizable LCE ink during DIW and the different elongated length of the printed LCEAs with an aligned printing path depending on the temperature (below or above the nematic-isotropic temperature). LCP (Vectra A950) was used in the other extrusion printing process (FFF), which uses solid filaments.<sup>15</sup> The molecular orientation of LCPs can be aligned with printing direction,

leading to the enhancement of the mechanical properties in the polymer structure. As shown in [Figure 6H](#), the nematic domains in LCP become highly aligned through the nozzle, caused by shear forces during the extrusion. However, the printed filament tends to lose its orientation and solidifies from the surface, leading to a core-shell microstructure with a highly aligned shell eventually. The mechanical properties of the printed hierarchical structure can be reinforced through thermal annealing to chemically crosslink the chain ends between filaments.

It is believed that, with the fast development of new 3D printing techniques, more functional applications will benefit from smart polymers. On the other hand, new applications will push the development of novel smart polymers and composites.

## APPLICATIONS

### AM in structural applications

There are increasing demands for new materials for functional products with desirable mechanical properties, such as ultra-lightweight or damage-tolerant structural materials for storage, micromechanical sensors, and biomedical devices. In the past, research has focused on the invention and modification of materials by manipulating chemical composition but, nowadays, microstructure design of materials in micro- and/or nanoscale is becoming mainstream. One of the alternatives is architected materials, which are multiphase materials whose microstructure and topology are controlled and optimized for physical properties that cannot be achieved with constituent materials alone. These benefits of the architected materials make them prospective materials, but the design complexity and multi-scale structure make them difficult to fabricate with conventional manufacturing techniques. 3D printing can be one of the manufacturing methods to overcome these challenges, which leads to the fabrication of novel materials.

#### *3D printing for producing architected materials with high stiffness and strength*

Materials with high specific strength (high strength but lightweight) are widely sought in aerospace, structural engineering, transportation, and tooling. Architected materials can exhibit light and enhanced stiffness and strength through the topological design and optimization. They are typically stretching-dominated structures that deform under uniaxial compression or tension. Some examples in [Figure 7](#) show the relationship between enhanced mechanical properties and their structural designs in micro- and nanoscale. A new class of plate nanolattices with the theoretical limit of stiffness and strength was developed using two-photon lithography and pyrolysis to create defect-free carbon.<sup>92</sup> To reach the theoretical stiffness and strength limits, a closed-cell plate structure with the integration of cubic and octet plates was applied. [Figure 7A](#) shows unit cell models and isometric scanning electron microscope (SEM) images of cubic + octet plate nanolattices with relative densities (i.e., the volume fraction of the solid constituent) from 25% to 60%. The nanolattices demonstrated the average performance improvements up to 639% over the best beam-nanolattices. Another example is high-entropy-alloy (HEA)-polymer composite octet-truss nanolattices that have high strength as well as high energy absorption via two-photon lithography.<sup>93</sup> The coating of metallic skins provided high specific stiffness and strength, and the trade-off between the strength and recoverability in materials could be alleviated by controlling local deformation, such as buckling or fracture, around the nodes with optimized material structure design. [Figure 7B](#) shows the structure of HEA-polymer composite nanolattices across five orders of magnitude in length scale from ~5 nm to ~100 μm. In a compression test of the composite nanolattices with 8–15 μm in core and 14.2 nm in HEA-coating thickness, the elastic buckling of the structure occurs from the

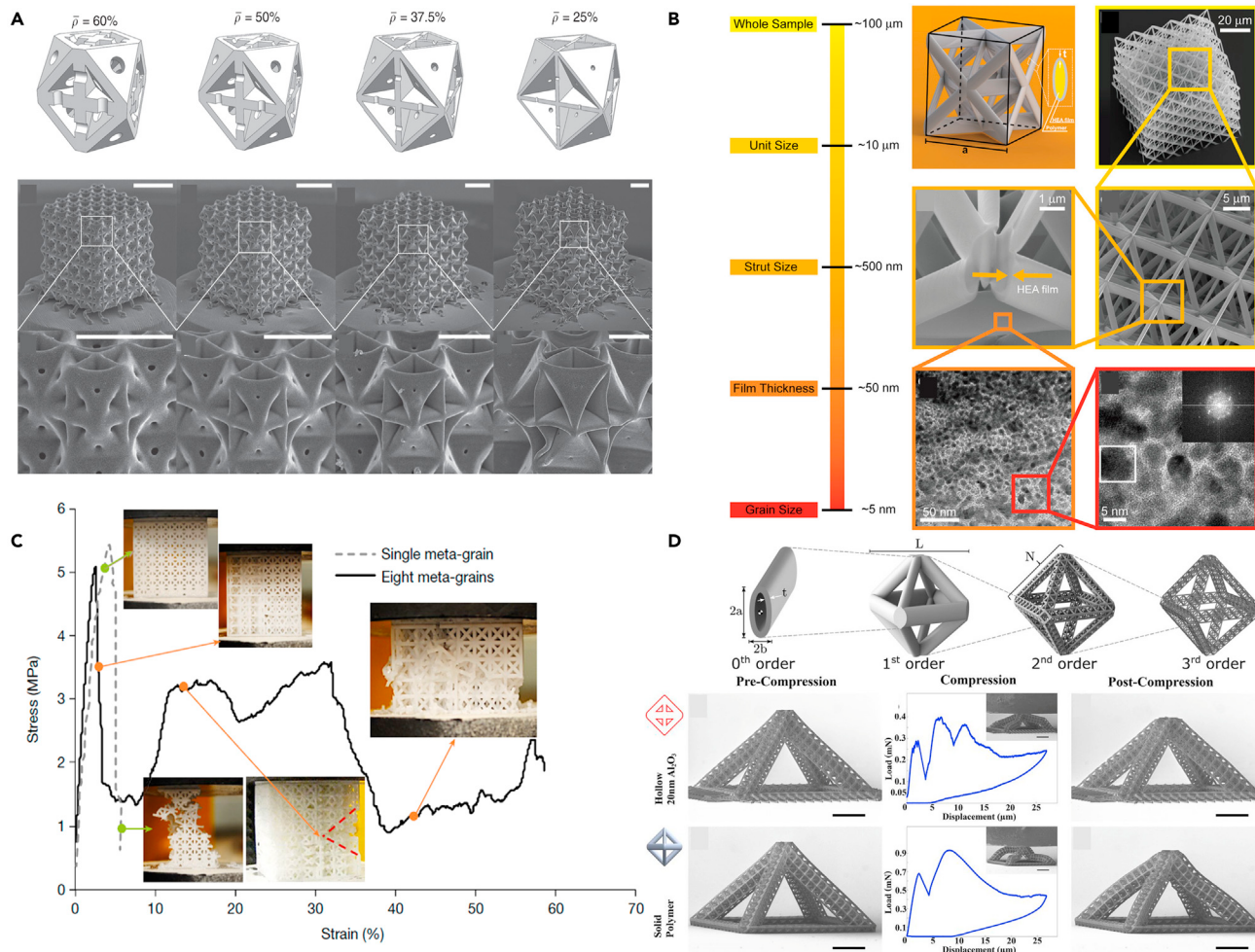


**Figure 7. 3D printing for structural applications**

(A) The unit cell models and isometric SEM images of cubic + octet plate nanolattices with different relative density (25%–60%) produced by two-photon lithography and subsequent pyrolysis. Reproduced with permission from Crook et al.<sup>92</sup> Copyright 2020, Springer Nature.

(B) The structure of HEA-polymer composite nanolattices across five orders of magnitude in length scale along with SEM images (yellow frames) and high-resolution transmission electron microscopy images (orange and red frames). Reproduced with permission from Zhang et al.<sup>93</sup> Copyright 2018, American Chemical Society.

(C) Stress-strain curve of the architected materials with boundaries between meta-grains that effectively stop cracks in the brittle lattice. Reproduced with permission from Pham et al.<sup>94</sup> Copyright 2019, Springer Nature.

(D) Upper: CAD images illustrating the process of creating a third-order hierarchical nanolattice. Lower: load displacement data that show compression to 50% strain with the images of the hollow 20 nm walled  $\text{Al}_2\text{O}_3$  sample and the polymer sample before and after compression. Reproduced with permission from Meza et al.<sup>95</sup> Copyright 2015, National Academy of Sciences.

bottom to the top allowing rotation and distortion around the struts without plastic deformation, resulting in nearly complete recovery on the unloading stage.

#### 3D printing for fabricating highly compliant materials

Besides the strength and stiffness, highly compliant materials with damage tolerance and high toughness are necessary to manage the extension of cracks in the structure and distribute and relieve stresses between adjacent parts. A high damage-tolerance-customized material using FFF was developed by mimicking the microscale crystalline structures.<sup>94</sup> Boundaries between meta-grains in brittle lattices enable the structure to prevent catastrophic collapse, resulting in enhanced toughness. The microstructure of these materials and compression test results are

shown in [Figure 7C](#). Different from the material composed of a single meta-grain, the material comprised of eight meta-grains with high-angle boundaries stops and deflects further crack propagation. Moreover, these boundaries help the architected materials to carry a load up to large deformation by improving the energy absorption. There are many other customized materials. One example is 3D hierarchical nanolattices fabricated using two-photon lithography, and they have high toughness and energy absorbent properties, attributed to hierarchically designed structures spanning multiple length scales.<sup>95</sup> [Figure 7D](#) exhibits CAD images of the process to make a third-order hierarchical nanolattice and the results of the compression tests on second-order octahedron of octet half-cells (hollow 20 nm walled Al<sub>2</sub>O<sub>3</sub> samples and polymer samples). In the compression test, the structures made of hollow ceramic showed post deformation (i.e., ductile); after unloading, they exhibited the highest average recovery up to 85%–98%, attributed to beam buckling in the first-order beams, shell buckling in the tubes, and microcracking at the nodes. Similarly, the polymer structures recovered up to 75%–90% of their original height, where the failure mechanism was primarily dominated by buckling in first- and second-order beams.

#### *Other metamaterials*

As shown in the above section, 3D printing techniques have produced new mechanical metamaterials through innovative geometric design. One kind of mechanical metamaterial, auxetic metamaterials, also can be created using 3D printing.<sup>96</sup> These materials have a negative Poisson's ratio, which is attractive for use in engineering applications, including sensors, actuators, and biomedical devices. In 2018, new hybrid auxetic metamaterials were created by a multi-material 3D printer. They have re-entrant core cells in the center of a basic chiral cell and expand their shape under a wide range of strain based on the concept of chirality-induced rotation.<sup>97</sup> As another example of 3D printed metamaterials, mesostructured materials are created via FFF.<sup>98</sup> These metamaterials have stochastic foams and are designed to have heterogeneous stiffness and anisotropic behavior that can change the kinematics of the robot. As envisioned in this section, the combination of 3D printing and metamaterials can create new research opportunities and benefit various fields.

#### **3D printing for biomedical applications**

In clinical medicine, tissue or organ transplantations using current approaches (e.g., auto-transplantation, xenotransplantation, and implantation of artificial organs) still have problems due to high cost, limited donors, and immunological rejection. Among the various methods of manufacturing artificial organs, 3D printing offers the opportunity to quickly create personalized tissues and organs using biocompatible polymers, including synthetic polymers (poly(ethylene glycol) diacrylate, PVA, poly(D,L-lactic-co-glycolic acid), PCL, and PLA) and natural polymers (gelatin methacrylate [GelMA], alginate, and collagen).<sup>99</sup> Different from the polymers for non-biomedical printing, polymers for 3D bioprinting should be biocompatible and have good mechanical and structural properties.

In bone tissue engineering scaffolds, scaffolds with appropriate structure (shape, pore size, and porosity), proper material properties (biocompatibility and degradability), mechanical properties, and desirable cellular interactions are required for regenerating engineering bone.<sup>100</sup> For example, bone tissue was fabricated with nano-hydroxyapatite/ PCL using SLS.<sup>77</sup> Different from conventional methods for scaffold fabrication, such as solution casting and injection molding, SLS allows rapid prototyping of complex geometrical scaffolds without the need for organic solvents, which can generate inflammation and toxic byproducts. The bone structure was

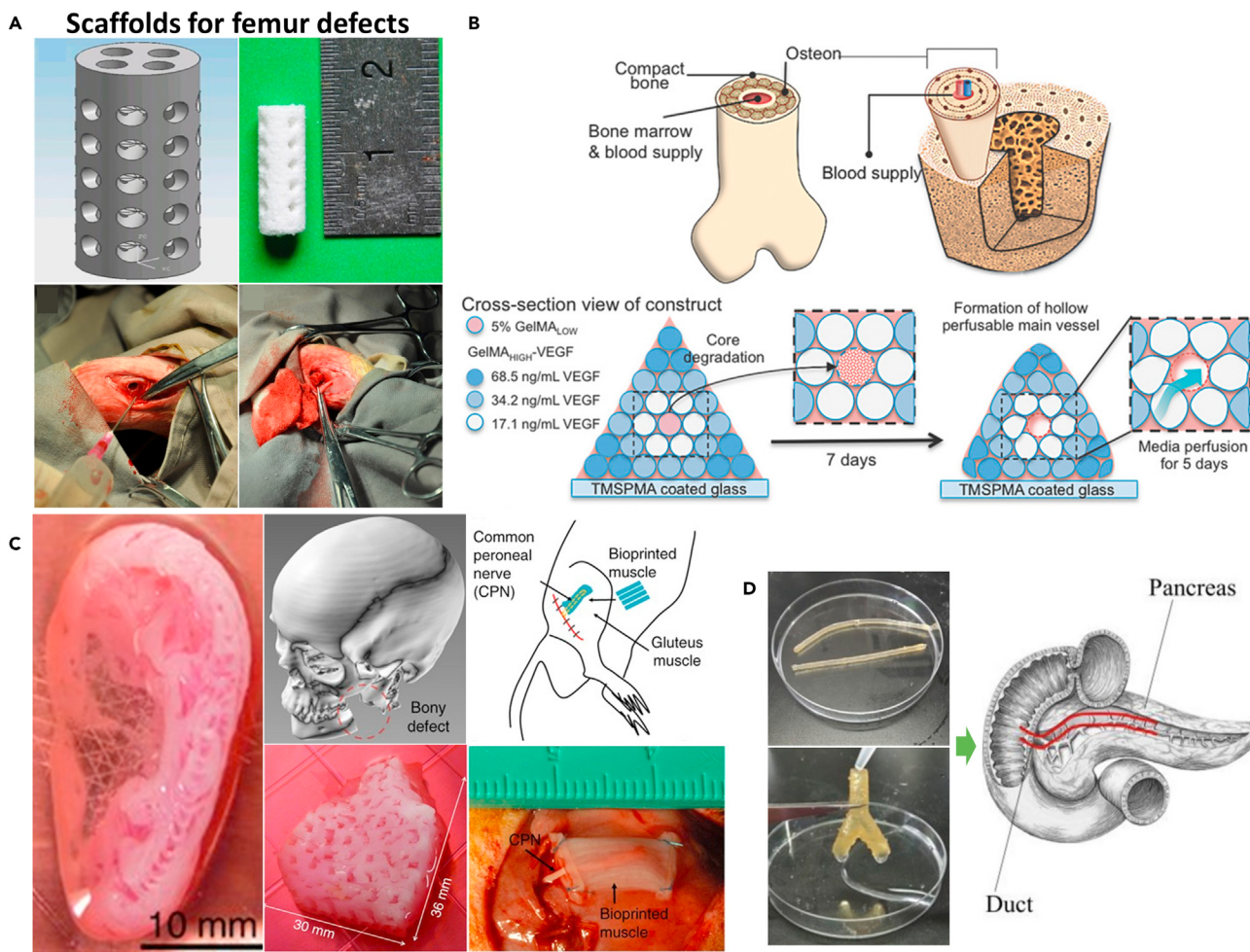


**Figure 8.** 3D printing for biological applications.

(A) Upper: CAD image of scaffolds for femur defect. Lower: image showing that the scaffolds were placed into the rabbit femur defect. Reproduced with permission from Xia et al.<sup>77</sup> Copyright 2013, Dove Medical Press.

(B) Upper: schematic illustration of the complex bone tissue structure. Lower: illustration of the bioprinting plan for manufacturing complex bone tissue structure. Individual rods of VEGF-functionalized GelMA bio-inks with different mechanical strength were printed out in a pyramidal structure. Reproduced with permission from Byambaa et al.<sup>101</sup> Copyright 2017, WILEY-VCH Verlag GmbH & Co.

(C) Images of bio-printed products to be implanted at the defects of humans and rats: ear, mandible bone, and muscle (from left to right). Reproduced with permission from Kang et al.<sup>102</sup> Copyright 2016, Springer Nature.

(D) Chitosan ducts for soft tissues produced by FDM. Reproduced with permission from Zhao et al.<sup>103</sup> Copyright 2020, Elsevier.

printed with the porous cylinder shape of scaffolds ranging in porosity from 78.54% to 70.31% and successfully implanted into rabbit femur defects, as shown in Figure 8B. These scaffolds showed good mechanical properties (1.98–3.17 MPa in compressive strength) and good biocompatibility.

Bioprinting using living cells together with biodegradable polymers leads to enormous development in biomedical applications. For example, engineering vascularized bone tissue was developed with bio-inks using an extrusion-based bio-printer.<sup>101</sup> As shown in Figure 8A, bone-mimicking 3D structures with osteogenic and vasculogenic niches were printed. The GelMA bio-inks were mixed with blood-derived human umbilical vein endothelial cells and bone marrow-derived human mesenchymal stem cells (hMSCs) for the development of a stable and robust vasculature network. In addition, different concentrations of vascular endothelial growth

factor (VEGF) were added to functionalized GelMA bio-ink to create a gradient of vasculogenesis. The middle part comprises a rapidly degradable GelMA in engineering bone tissue, which was designed to degrade to form a hollow main vessel. The outer layers were printed using bio-ink with three different concentrations of VEGF to induce osteogenic differentiation of hMSCs into osteoblasts. On the other hand, a new 3D printer combining jetting, extrusion, and laser-induced forward transfer was developed for manufacturing bone, cartilage, and skeletal muscle.<sup>102</sup> The integrated 3D printer was optimized for printing multiple-sized bio-constructions with sufficient structural integrity. The bioprinting was conducted using a specific concentration of cell-laden hydrogels, sacrificial acellular hydrogel, and PCL polymer, which was used as supporting material. Figure 8C shows several pictures of 3D printed tissues and organs: ear, mandible bone, and muscle. This bioprinting shows the feasibility of printing living tissue structures with appropriate strength.

Also, fibrin, a fibrous protein, has been applied in medical engineering for various tissues (e.g., skin, vessels, and bone), and their blends are used in both scaffold and scaffold-free technologies.<sup>78</sup> With the development of bioprinting, fibrin-based bio-inks have been widely used as feedstocks due to their unique biocompatible, biodegradable, and benign properties. With such bio-inks, artificial skin, heart, and neural constructs can be printed.

Soft tissues, such as nerves, blood vessels, and fibrous tissues, are also actively studied using 3D printing technologies. Figure 8D shows ducts produced by different printing methods: a combination of the rotary axis and a DIW, and a combination of FFF and DIW.<sup>103</sup> In this study, natural polymer (chitosan) and degradable biopolymers (PLA) were used for printing. Chitosan was used as the main component in artificial ducts, and PLA was used to support the chitosan ducts. The printed ducts exhibited satisfactory mechanical properties (tensile strength, Young's modulus, and fracture strain) matching the soft tissue, which can replace pancreatic ducts.

### 3D printing for electrochemical energy storage

Since the discovery of electricity, numerous technologies have been studied for the effective storage of electrical energy. Among them, electrochemical energy storage (EES) technology is essential for building resilient energy systems. In the past, most academic research focused on synthesizing new materials for the components of EES devices, such as electrodes, electrolytes, and separators. However, researchers have discovered that the structure and multiple sizes of the components also play a critical role in the performance of EES devices, even outperforming their bulk structure. More attention is being paid to the architecture of the EES devices in recent years.

3D printing has been widely applied in the energy storage field due to its simple process, geometric flexibility, and ability to print multi-scale structures. For example, a micro-lattice cathode made of sulfur copolymer-graphene (3DP-pSG) was fabricated using DIW and simple thermal treatment via a facile copolymerization between elemental sulfur and polymer, as shown in Figure 9A.<sup>104</sup> The printing ink for DIW printing is composed of S particles, 1,3-diisopropenylbenzene, and condensed GO dispersion, and DIW technology allows rapid and accurate fabrication of a porous cathode structure that facilitates ion movement. Also, the strong covalent bond between polymer and sulfur in the 3DP-pSG can suppress the dissolution of polysulfides and show better specific capacity than a 3D printed sulfur-graphene cathode without polymer (3DP-SG) in overall cycle performance with a current density range of 50–800 mA·g<sup>-1</sup>.

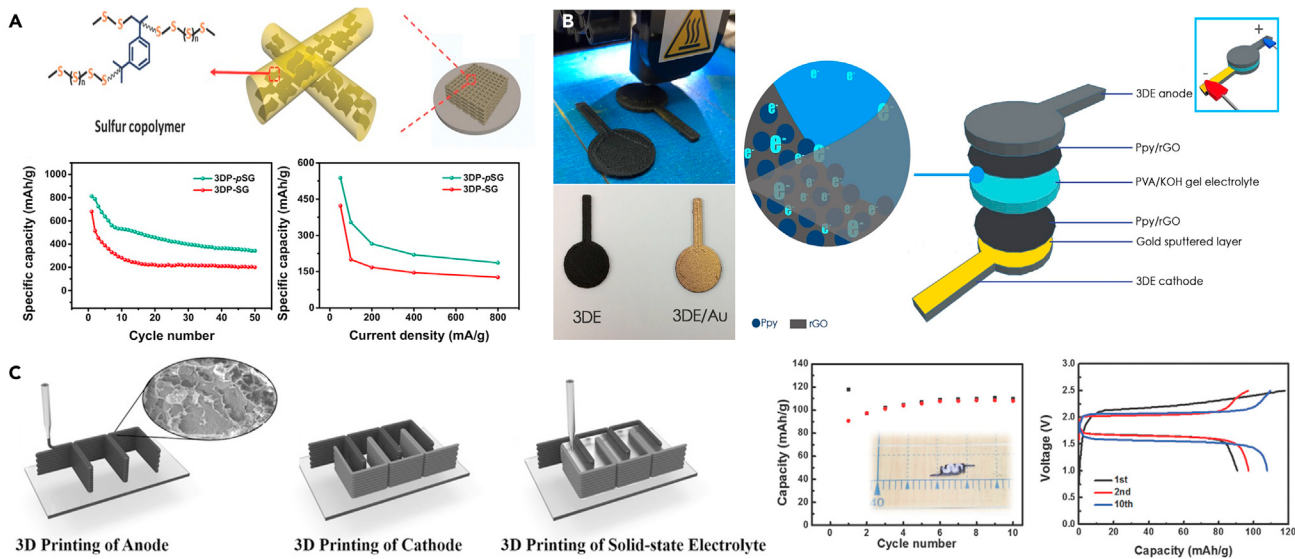


**Figure 9. 3D printing for energy storage materials and devices**

(A) Schematic of 3D printed sulfur copolymer-graphene (3DP-pSG) architectures and electrochemical characterization of batteries with 3DP-pSG: cycle performances of 3DP-pSG and 3DP-SG at  $50 \text{ mA g}^{-1}$  and rate capabilities of 3DP-pSG and 3DP-SG at a current density range of  $50\text{--}800 \text{ mA g}^{-1}$ . Reproduced with permission from Shen et al.<sup>104</sup> Copyright 2017, WILEY-VCH Verlag GmbH & Co.

(B) Schematic of a solid-state supercapacitor with 3D printed electrodes sputtered with gold. Reproduced with permission from Foo et al.<sup>74</sup> Copyright 2018, Springer Nature.

(C) Left: schematic of the 3D-printed interdigitated electrodes using LTO/rGO ink, LFP/rGO ink, and polymer composite ink. Right: cycling stability and charge and discharge profiles of the 3D-printed full cell, composed of LFP/rGO, LTO/rGO, and polymer composite electrolyte. Reproduced with permission from Fu et al.<sup>105</sup> Copyright 2016, WILEY-VCH Verlag GmbH & Co.

Another example is graphene-based electrodes using a simple FFF method, which can reduce cost and time and provide an environmentally friendly approach.<sup>74</sup> Figure 9B shows the schematic of a solid-state supercapacitor with 3D printed electrodes and a PVA-KOH gel electrolyte sandwiched between them. The thin layer of gold was sputtered onto the 3D printed electrodes' surface for reducing the surface resistivity. The supercapacitor with the printed electrodes exhibited good capacitance performance over a potential range of  $+0.0\text{--}1.0 \text{ V}$  at a scan rate of  $50 \text{ mVs}^{-1}$  and good cycling stability over 100 cycles. The other example utilizing extrusion-based 3D printing is all-component 3D-printed lithium-ion batteries.<sup>105</sup> As shown in Figure 9C, the anode and cathode were fabricated using LTO/rGO ink and LFP/rGO ink, respectively. After annealing the electrodes, the solid-state gel polymer ink containing a mixture of poly(vinylidene fluoride)-co-hexafluoropropylene and alumina oxide ( $\text{Al}_2\text{O}_3$ ) nanoparticles was injected between the electrodes. The batteries were printed with interdigitated architecture and showed a capacity of  $\sim 100 \text{ mAhg}^{-1}$  in 10 cycles at a specific current of  $50 \text{ mA g}^{-1}$ . The initial charge and discharge capacities were  $117$  and  $91 \text{ mAhg}^{-1}$ , respectively; in the following cycles, they slightly increased, and in the 10th cycle, the capacities reached  $110$  and  $108 \text{ mAhg}^{-1}$ , showing nearly 100% of columbic efficiency.

### 3D printing for electronics

The advantages of 3D printing, including rapid prototyping and design flexibility, can speed up innovation in diverse industries. By adding conductive materials such as carbon nanotube and metal nanoparticles in feedstocks, the polymer composites can be readily used as electronic components. In recent years, with the increasing interest in wearable electronics, soft robots, and stretchable electronics, 3D printing of electronics

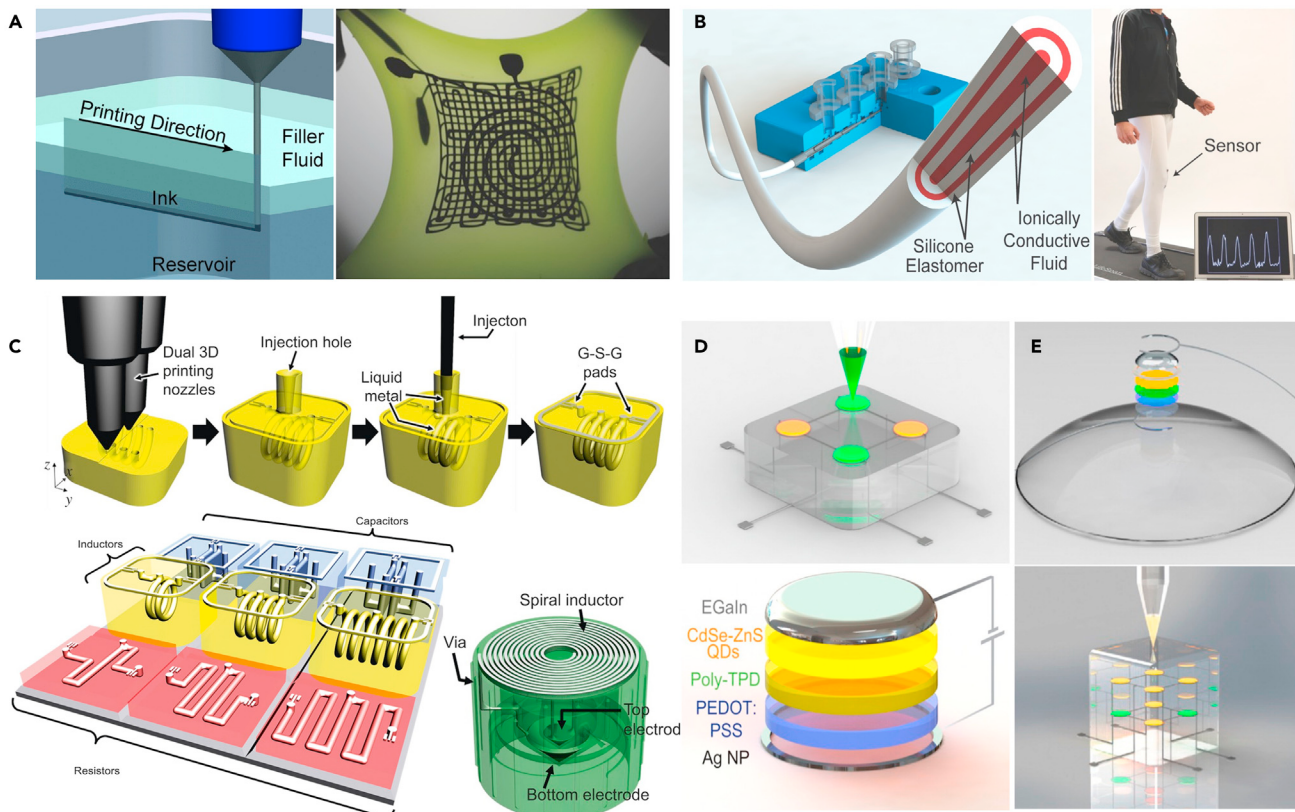


**Figure 10. 3D printing for electronics**

(A) Schematic of embedded 3D printing and photograph of the 3D printed stretchable strain sensor at a stretched state. Reproduced with permission from Muth et al.<sup>106</sup> Copyright 2014, Wiley-VCH Verlag GmbH & Co.

(B) Schematic illustration of multicore-shell printing for a capacitive soft strain sensor (CS3), and textile CS3 attached to fabric across the knee to demonstrate the application of the CS3 as a wearable sensor. Reproduced with permission from Frutiger et al.<sup>108</sup> Copyright 2015, WILEY-VCH Verlag GmbH & Co.

(C) Upper: illustration of 3D printing methods, including the filling of liquid metal paste for producing microelectronic components, circuitries, and a passive wireless sensor. Lower: 3D integrated microelectronic components, including capacitors, solenoid-type inductors, and resistors and a passive wireless sensor containing resonant (LC) circuits. Reproduced with permission from Wu et al.<sup>107</sup> Copyright 2015, Springer Nature.

(D) Schematic illustration of direct 3D printing of QD-LEDs. Reproduced with permission from Kong et al.<sup>110</sup> Copyright 2014, American Chemical Society.

(E) 3D printing QD-LEC components on various substrates (curvilinear substrate and inside cube structure). Reproduced with permission from Kong et al.<sup>110</sup> Copyright 2014, American Chemical Society.

has been actively researched because 3D printing can manufacture custom-shaped multifunctional electronics, such as stretchable electronics with functional elements (e.g., sensors, circuits, and other embedded components,<sup>106,107</sup> embedded electronics,<sup>108</sup> and structural electronics<sup>109</sup>). For example, highly stretchable sensors were developed using embedded 3D printing of carbon-based ink.<sup>106</sup> The embedded 3D printing inside the elastomeric matrix can create mechanically robust flexible sensors, which can sense mechanical deformation through the change of electrical resistance. Figure 10A exhibits the embedded 3D printing process and an image of the strain and pressure sensor in the stretched state, along with the schematic of the printing method. The sensors are another example of 3D printing of electronics, and soft strain sensors were manufactured using multicore-shell printing.<sup>108</sup> The sensors were made by extruding ionically conductive fluid (composed of glycerol, sodium chloride, and polyethylene glycol) and a silicone elastomer with coaxially aligned nozzles. Figure 10B shows the schematic of the sensor, and it can work as a capacitive sensor owing to

the stretchable ionically conductive fluid and dielectric elastomer. Both are examples of embedded conductive materials into elastic polymers using 3D printing and can be used in wearable electronics, such as clothes and shoe insoles, by integrating with textiles.

The development of portable electronic devices calls for increasing demand for miniaturization and customization of electronic components. 3D printing enables the fabrication of structural electronics by customizing their shape and size for desired applications. For instance, the microelectronics components and circuits were produced by FFF.<sup>107</sup> Figure 10C gives a 3D structure with hollow microchannels printed in FFF and then filled with liquid metal paste. The printed devices can be formed as an integrated system within an arbitrary 3D structure. A 3D printing for seamless integration of diverse materials on a 3D surface has been shown using direct ink printing and 3D scanning of surface topologies.<sup>110</sup> Figure 10D shows quantum dot-based light-emitting diodes (QD-LEDs), fully integrated into device components with active properties, printed by direct ink printing. The layer by layer process of 3D printing enables the fabrication of encapsulated active electronics, such as multidimensional array of embedded QD-LEDs 3D, and when direct ink printing is combined with 3D scanning technology materials can be printed on a variety of substrates, including curvilinear surfaces, as shown in Figure 10E. Similar to the printed structural electronics above, there are advanced versions of electronics that can be assembled into blocks of multiple units to provide a variety of electromechanical connections and functions. These digital materials, called Bitbloxs, were printed using a modified personal 3D printer based on MJ.<sup>111</sup> The single Bitbox is less than 1 cm, and it can be simply assembled using thruhole pin-and-socket connectors. If the Bitbox form-factor combines with DC motors, a low-cost leadscrew actuator can be made.

### 3D printing for robotics

As discussed above, 3D printing can deliver customized products with complex geometry in a fast and cost-effective way. It also offers a wide selection of materials, such as polymers and composites with diverse properties (strength, stiffness, chemical resistance, etc.). With these advantages, 3D printing meets the current requirements for robotics applications. Limited by available manufacturing techniques, conventional robotics are accomplished by assembling multiple components, which consumes lots of time. 3D printing provides solutions to overcome the engineering challenges in robot fabrication by eliminating custom molds and multiple assembly steps. Even in industry, engineers are actively using 3D printing for robotics. One example is the fabrication of robot grippers, which are expensive to fabricate and require intensive customization for different applications. Printing these parts allows the components to have a lightweight, compact design, rather than the traditional heavy, non-customized designs, resulting in improved performance, such as faster movement and higher load. Haddington Dynamics, for example, is utilizing 3D printers to fabricate robot arms, including a gripper for NASA and GoogleX.

Soft robots have received tremendous attention due to their ability to perform complex movements even in a harsh or uncertain environment. The development of 3D printing techniques and advances of functional soft materials facilitate the fabrication of soft robots that are mostly inspired by biology, which has been optimized over millions of years. For example, a frog robot, which can jump with combustion power, was fabricated using a MJ 3D printing technique, as shown in Figure 11A.<sup>112</sup> The stiffness gradient of the robot body facilitates its body transitions from a rigid core to a soft exterior by reducing stress at the interface of materials mismatched in compliance. As another example, a hydraulically actuated hexapod robot can be made using MJ.<sup>113</sup> All components of the hexapod robot were printed in a single

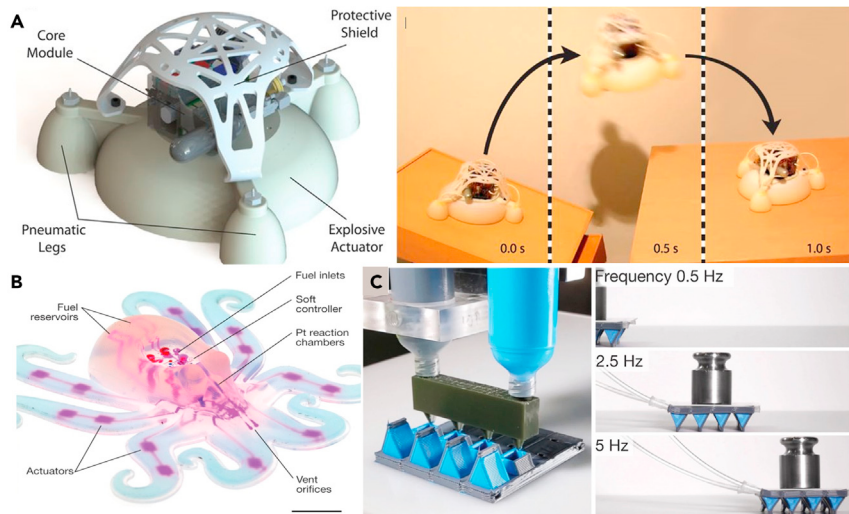


**Figure 11. 3D printing for robotics applications**

(A) Image of a robot consisting of the pyrotechnic actuator surrounded by three pneumatic legs. A rigid core structure that contains power and control components in a semisoft shield. And the photograph of performance that the robot jumps off an angled surface onto a table. Reproduced with permission from Bartlett et al.<sup>112</sup> Copyright 2015, American Association for the Advancement of Science.

(B) Images of a fully soft, autonomous robot (octobot) controlled by the embedded microfluidic soft controller and powered by monopropellant decomposition. Reproduced with permission from Wehner et al.<sup>114</sup> Copyright 2016, Springer Nature.

(C) Schematic of a soft robotic millipede walker and its movement. The walker is composed of the flexible silicone acting like muscles and the stiff silicone for the displacement produced by an advanced DIW technique (MM3D printing). It has pneumatic actuators that connect the two-channel networks, and the walking speed can be controlled by frequency. Reproduced with permission from Skylar-Scott et al.<sup>41</sup> Copyright 2019, Springer Nature.

step of MJ. Using different materials (photopolymers and non-curing liquid), the fluidic channels in the hexapod robot were fabricated, and the channels were used for hydraulically actuated movement of the robot.

Another example using advanced 3D printing is an octopus robot, which is called octobot.<sup>114</sup> Figure 11B shows the key components and schematic of an octobot. The shape of the octobot was produced by molding of PDMS, and the pneumatic networks were manufactured using an embedded 3D printing technique. The octobot can move because there is a controlled microfluidic system that can generate gas and make downstream fluid flow upon catalytic decomposition of fuel. A soft robotic millipede walker is also a good example that was created using an advanced DIW technique—multi-material multi-nozzle 3D printing.<sup>41</sup> As described in “ME”, it employed a high switching frequency for multi-material printing. The printed walker consisted of flexible and stiff silicone by depicting the muscles and the legs, respectively, as shown in Figure 11C. The robot has pneumatic actuators, and it moves when the soft silicone muscle buckles, causing lateral and vertical displacement of the stiff leg. The speed of the robot depends on actuator frequency.

More recently, mechanical metamaterials have changed the functional paradigm in robotics. As one example, pneumatic actuators that buckle when interior pressure is less than exterior pressure were developed by 3D printing of elastomers.<sup>113</sup> These

actuators consisted of a non-buckling center area connecting to several buckling pillars. The misalignment of the pillars relative to the center area makes the center area rotate. They can be used as a soft gripper, and their use on robots offers many advantages, such as being lightweight and safe. Furthermore, the use of metamaterials in combination with smart materials, such as SMPs, could enable robots to move without batteries or on-board electronics.<sup>115</sup> The power for actuation can be obtained from the SMP muscle or the designed bistable element.

### PERSPECTIVE AND CONCLUSIONS

As discussed in this review, 3D printing techniques have progressed along with new processing techniques and functional polymers, which are reshaping the manufacturing industry and will benefit our society. As the resolution of 3D printing approaches nanoscale,<sup>116,117</sup> diverse application fields can obtain new opportunities to manufacture high-performance products with multi-scale optimized structure and function. Furthermore, if we design the chemical and physical properties of polymers at an early stage, we can activate shape changing and control the motion of the printed products. Although AM technologies are becoming mature and have provided new insight and opportunities in various fields, several limitations still need to be overcome. If we use them as guidelines for further studies, they can offer new opportunities and possibilities for novel polymer development and applications. Here, we list some critical challenges that should be addressed in future research.

- (1) Diversity of materials. AM processes grow based on the development of polymers, but there is still a limited choice of printable materials due to the requirements for printing, such as rheology, melting point, and other physical properties. For instance, polymers with low melting temperatures and appropriate viscosity are widely used in FFF; but these materials often result in unsatisfying mechanical and chemical properties of final products. In the case of products made of photopolymer, they are usually brittle due to the properties of constituent materials. More research is needed for engineering-grade polymers to meet the demands in aerospace, automobile, and structural applications. On the other hand, diverse functionalities should be considered in polymers and polymer composites for AM, leveraging the synergistic effect of shape and functions in a whole part. In this direction, biology systems and biomaterials will inspire materials development, function innovation, and structure design.
- (2) Enhancement of AM processes for high-quality prints. The printing processes can generate flaws inside the printed products, leading to deteriorated mechanical properties of 3D printed products and discrepancies between parts and digital models. Therefore, understanding where the main defects are coming from and how to deal with these flaws is important. One of the major drawbacks of 3D printing is void formation in printed objects. These are critical problems in PBF and BJ since the shape of powder can easily create void during printing caused by unsatisfied bonding between melted materials and binder. In addition, weak bonding between layers of manufactured parts should be improved. This unsatisfactory bonding induces anisotropic and inferior mechanical properties at the perpendicular direction of the printed layer and can potentially cause delamination between layers. There are lots of trials to overcome these limitations, such as adding fillers and using laser or IR lamps to generate heat between the printed layers. Emerging techniques, such as volumetric manufacturing,<sup>43</sup> can potentially address such

- problems. Besides, *in situ* monitoring and post-inspection are necessary for better quality control.
- (3) High-throughput and scalable manufacturing. Most 3D printing technologies are slow during the printing stage, and additional post-processing can further reduce the throughput and scalability. The industry is trying to produce large-scale products by applying a robot arm to the FFF that is not restricted by the printing plate. In terms of post-processing, chemical or water-soluble materials are used as support in FFF to save time for support cleaning. Moreover, some AM techniques are limited to small builds and low throughput, because printing large parts quickly would generate excessive heat, which distorts final products. These issues prohibit their adoption by industry. These days, some research has been done for high productivity by controlling heat generation using mobile oil.<sup>44</sup> Meanwhile, new printing concepts, such as volumetric AM,<sup>43</sup> are becoming a new trend. In addition, inconsistent printing might be another factor hindering the scalability of AM. Feedback systems, such as machine learning-powered inspection systems, should be integrated and studied for better repeatability in scalable manufacturing.<sup>118</sup>
- (4) Multi-material and multi-scale AM for a variety of applications. The multi-material with multi-scale manufacturing technique is essential for simultaneously controlling not only material composition and ratio and functions but also internal architecture at the micro- and nanoscale. Objects created for biological, electronic, and robotic applications usually require multiple materials of varying scale to have a series of complex movements or multiple components for specific reactions. The development of multi-material and multi-scale AM will be a game-changing technique for various fields to eliminate material waste and assembly steps. However, some 3D printing techniques have difficulty printing multiple materials. In the case of VP, multiple reservoirs might be needed for printing multi-materials. As one of the alternative methods, a rotating vat carousel system to automatically change the material has been invented.<sup>119</sup> Recently, a microfluidic system has been employed in VP for multilateral printing.<sup>48</sup> This multi-material 3D microprinting has been developed based on a commercial 3D direct laser writing technique and additionally has a microfluidic chamber and an electronic pressure controller to automatically fill and replace material in the microchamber. Although it demonstrates advances in composite printing, the height of structures capable of 3D printing is limited due to the microchamber size. Also, in terms of materials, it is difficult to fabricate products with high loading of reinforcements due to limited printing capability. For example, in FFF techniques, if a high content of fillers is added to the polymer, the particle clustering makes filaments brittle, resulting in clogged nozzles. In the long term, hybrid AM can be a trend to meet various customized requirements. We envision that the 3D printing of a robot that can walk off the printing plate will become true in the near future.
- (5) Safety issues. With the increasing interest and adoption of AM, safety issues have been mentioned continuously. Polymer-based AM can generate not only particulate matters (PM),<sup>120,121</sup> but also volatile organic compounds (VOCs) such as toluene, aldehydes, and ethylbenzene.<sup>121,122</sup> For example, the most popular thermoplastics (ABS and PLA) have been found to release VOCs.<sup>123</sup> For safe printing, chemical reactions and corresponding emission of fumes in manufacturing stages must be controlled. Detailed studies about the formation mechanism of PM and VOC in different printing methods will lead to more environmentally friendly printer design and sophisticated control and personal protection strategies.

(6) Sustainability. Striving for a sustainable future, reducing and handling waste should be studied in AM. One of the methods to make AM eco-friendly is the improvement of biodegradable polymers and the replacement of oil-based feedstocks with bio-based compostable plastics.<sup>124</sup> Another approach is the management of failed prints and end-of-life products through recycling. Recycling waste plastics can reduce material costs and decrease demand for the frequent resupply of parts by the supply chain. Thermoplastics are easily recyclable compared with thermosets due to no or low degradation of the polymer chain when melted down. In thermoplastics, the weaker interactions between polymer chains break, whereas in thermosets, the bonds between monomers are broken, and their properties deteriorate each time they are reused, making it much more difficult to recycle thermoset polymers. One example of thermoplastic recycling is processing of polyethylene terephthalate bottles and packaging them into filaments for 3D printing.<sup>125</sup> The recycled filament has the capability for replacing commercial filaments by showing comparable tensile strength and elongation. Finally, in other 3D printing, such as PBF and VP, research on the reuse of unused materials (powder and resin, respectively) is being conducted.

## ACKNOWLEDGMENTS

This work is supported by the University of Delaware startup funding.

## AUTHOR CONTRIBUTIONS

Writing – original draft, S.P.; writing – review & editing, S.P., W.S., L.M., and W.M.; supervision, W.S., and K.F.

## DECLARATION OF INTERESTS

The authors declare no competing interests.

## REFERENCES

1. Spadaccini, C.M. (2019). Additive manufacturing and processing of architected materials. *MRS Bull.* **44**, 782–788.
2. Greer, J.R., and Deshpande, V.S. (2019). Three-dimensional architected materials and structures: design, fabrication, and mechanical behavior. *MRS Bull.* **44**, 750–757.
3. Sydney Gladman, A., Matsumoto, E.A., Nuzzo, R.G., Mahadevan, L., and Lewis, J.A. (2016). Biomimetic 4D printing. *Nat. Mater.* **15**, 413–418.
4. Feldman, D. (2008). Polymer history. *Des. Monomers Polym.* **11**, 1–15.
5. Wohlers, T., and Gornet, T. (2016). History of Additive Manufacturing (Wohlers Report.).
6. Zhang, Q., Zhang, K., and Hu, G. (2016). Smart three-dimensional lightweight structure triggered from a thin composite sheet via 3D printing technique. *Sci. Rep.* **6**, 1–8.
7. Van Manen, T., Janbaz, S., and Zadpoor, A.A. (2017). Programming 2D/3D shape-shifting with hobbyist 3D printers. *Mater. Horizons* **4**, 1064–1069.
8. Long, K.N., Scott, T.F., Jerry Qi, H., Bowman, C.N., and Dunn, M.L. (2009). Photomechanics of light-activated polymers. *J. Mech. Phys. Sol.* **57**, 1103–1121.
9. Wei, H., Zhang, Q., Yao, Y., Liu, L., Liu, Y., and Leng, J. (2017). Direct-write fabrication of 4D active shape-changing structures based on a shape memory polymer and its nanocomposite. *ACS Appl. Mater. Interfaces* **9**, 876–883.
10. Schwartz, J.J., and Boydston, A.J. (2019). Multimaterial actinic spatial control 3D and 4D printing. *Nat. Commun.* **10**, 1–10.
11. Raviv, D., Zhao, W., McKnelly, C., Papadopoulou, A., Kadambi, A., Shi, B., Hirsch, S., Dikovsky, D., Zyracki, M., Olgun, C., et al. (2014). Active printed materials for complex self-evolving deformations. *Sci. Rep.* **4**, 1–9.
12. Van Oosten, C.L., Bastiaansen, C.W.M., and Broer, D.J. (2009). Printed artificial cilia from liquid-crystal network actuators modularly driven by light. *Nat. Mater.* **8**, 677–682.
13. Yuan, C., Roach, D.J., Dunn, C.K., Mu, Q., Kuang, X., Yakacki, C.M., Wang, T.J., Yu, K., and Qi, H.J. (2017). 3D printed reversible shape changing soft actuators assisted by liquid crystal elastomers. *Soft Matter* **13**, 5558–5568.
14. Kotikian, A., Truby, R.L., Boley, J.W., White, T.J., and Lewis, J.A. (2018). 3D printing of liquid crystal elastomeric actuators with spatially programmed nematic order. *Adv. Mater.* **30**, 1706164.
15. Ganterbein, S., Masania, K., Woigk, W., Sesseg, J.P.W., Tervoort, T.A., and Studart, A.R. (2018). Three-dimensional printing of hierarchical liquid-crystal-polymer structures. *Nature* **561**, 226–230.
16. Rim, Y.S., Bae, S.H., Chen, H., De Marco, N., and Yang, Y. (2016). Recent progress in materials and devices toward printable and flexible sensors. *Adv. Mater.* **28**, 4415–4440.
17. Mao, S., Dong, E., Jin, H., Xu, M., and Low, K.H. (2016). Locomotion and gait analysis of multi-limb soft robots driven by smart actuators. *IEEE Int. Conf. Intell. Robot. Syst.* **2016**, 2438–2443.
18. Gao, B., Yang, Q., Zhao, X., Jin, G., Ma, Y., and Xu, F. (2016). 4D bioprinting for biomedical applications. *Trends Biotechnol.* **34**, 746–756.
19. Drummer, D., Medina-Hernández, M., Drexler, M., and Wudy, K. (2015). Polymer powder production for laser melting through immiscible blends. *Proced. Eng.* **102**, 1918–1925.
20. Schmid, M., Amado, A., and Wegener, K. (2015). Polymer powders for selective laser

- sintering (SLS), 1664. In AIP Conference Proceedings, p. 691.
21. Mokrane, A., Boutaous, M., and Xin, S. (2018). Process of selective laser sintering of polymer powders: modeling, simulation, and validation. *Comptes Rendus Mec.* 346, 1087–1103.
  22. Schawe, J.E.K. (2016). Cooling rate dependence of the crystallinity at nonisothermal crystallization of polymers: a phenomenological model. *J. Appl. Polym. Sci.* 133, 1–7.
  23. Gu, H., AlFayez, F., Ahmed, T., and Bashir, Z. (2019). Poly(ethylene terephthalate) powder—a versatile material for additive manufacturing. *Polymers* 11, 2041.
  24. Ni, R., Qian, B., Liu, C., Liu, X., and Qiu, J. (2018). A cross-linking strategy with moderated pre-polymerization of resin for stereolithography. *RSC Adv.* 8, 29583–29588.
  25. Bagheri, A., and Jin, J. (2019). Photopolymerization in 3D printing. *ACS Appl. Polym. Mater.* 1, 593–611.
  26. Khalina, M., Beheshty, M.H., and Salimi, A. (2019). The effect of reactive diluent on mechanical properties and microstructure of epoxy resins. *Polym. Bull.* 76, 3905–3927.
  27. Peng, S., Li, Y., Wu, L., Zhong, J., Weng, Z., Zheng, L., Yang, Z., and Miao, J.T. (2020). 3D printing mechanically robust and transparent polyurethane elastomers for stretchable electronic sensors. *ACS Appl. Mater. Interfaces* 12, 6479–6488.
  28. Lewis, J.A. (2006). Direct ink writing of 3D functional materials. *Adv. Funct. Mater.* 16, 2193–2204.
  29. Wang, X., Jiang, M., Zhou, Z., Gou, J., and Hui, D. (2017). 3D printing of polymer matrix composites: a review and prospective. *Compos. Part. B Eng.* 110, 442–458.
  30. Kazmer, D. (2017). Three-dimensional printing of plastics. In *Applied Plastics Engineering Handbook: Processing, Materials, and Applications*, Second Edition, Myer Kutz, ed. (Elsevier Inc.), pp. 617–634.
  31. Turner, B.N., Strong, R., and Gold, S.A. (2014). A review of melt extrusion additive manufacturing processes: I. Process design and modeling. *Rapid Prototyp. J.* 20, 192–204.
  32. Venkataraman, N., Rangarajan, S., Matthewson, M.J., Harper, B., Safari, A., Danforth, S.C., Wu, G., Langrana, N., Gucer, S., and Yardimci, A. (2000). Feedstock material property—process relationships in fused deposition of ceramics (FDC). *Rapid Prototyp. J.* 6, 244–252.
  33. Luo, M., Tian, X., Zhu, W., and Li, D. (2018). Controllable interlayer shear strength and crystallinity of PEEK components by laser-assisted material extrusion. *J. Mater. Res.* 33, 1632–1641.
  34. Kishore, V., Ajinjeru, C., Nycz, A., Post, B., Lindahl, J., Kunc, V., and Duty, C. (2017). Infrared preheating to improve interlayer strength of big area additive manufacturing (BAAM) components. *Addit. Manuf.* 14, 7–12.
  35. Sweeney, C.B., Lackey, B.A., Pospisil, M.J., Achee, T.C., Hicks, V.K., Moran, A.G., Teipel, B.R., Saed, M.A., and Green, M.J. (2017). Welding of 3D-printed carbon nanotube-polymer composites by locally induced microwave heating. *Sci. Adv.* 3, 1–7.
  36. Ching, T., Li, Y., Karyappa, R., Ohno, A., Toh, Y.C., and Hashimoto, M. (2019). Fabrication of integrated microfluidic devices by direct ink writing (DIW) 3D printing. *Sensors Actuators B Chem.* 297, 126609.
  37. Guo, S.-Z., Qiu, K., Meng, F., Park, S.H., and McAlpine, M.C. (2017). 3D printed stretchable tactile sensors. *Adv. Mater.* 29, 1701218.
  38. Hinton, T.J., Jallerat, Q., Palchesko, R.N., Park, J.H., Grodzicki, M.S., Shue, H.J., Ramadan, M.H., Hudson, A.R., and Feinberg, A.W. (2015). Three-dimensional printing of complex biological structures by freeform reversible embedding of suspended hydrogels. *Sci. Adv.* 1, e1500758.
  39. Malda, J., Visser, J., Melchels, F.P., Jüngst, T., Hennek, W.E., Dhert, W.J.A., Groll, J., and Hutmacher, D.W. (2013). 25th anniversary article: engineering hydrogels for biofabrication. *Adv. Mater.* 25, 5011–5028.
  40. Xie, B., Parkhill, R.L., Warren, W.L., and Smay, J.E. (2006). Direct writing of three-dimensional polymer scaffolds using colloidal gels. *Adv. Funct. Mater.* 16, 1685–1693.
  41. Skylar-Scott, M.A., Mueller, J., Visser, C.W., and Lewis, J.A. (2019). Voxelized soft matter via multimaterial multinozzle 3D printing. *Nature* 575, 330–335.
  42. Tumbleston, J.R., Shirvanyants, D., Ermoshkin, N., Januszewicz, R., Johnson, A.R., Kelly, D., Chen, K., Pinschmidt, R., Rolland, J.P., Ermoshkin, A., et al. (2015). Continuous liquid interface production of 3D objects. *Science* 347, 1349–1352.
  43. Kelly, B.E., Bhattacharya, I., Heidari, H., Shusteff, M., Spadaccini, C.M., and Taylor, H.K. (2019). Volumetric additive manufacturing via tomographic reconstruction. *Science* 363, 1075–1079.
  44. Walker, D.A., Hedrick, J.L., and Mirkin, C.A. (2019). Rapid, large-volume, thermally controlled 3D printing using a mobile liquid interface. *Science* 366, 360–364.
  45. Schmidlein, C., and Kalaskar, D.M. (2018). Stereolithography. In *3D Printing*, Dragan Cvetković, ed. (InTech), pp. 1–22.
  46. Manapat, J.Z., Chen, Q., Ye, P., and Advincola, R.C. (2017). 3D printing of polymer nanocomposites via stereolithography. *Macromol. Mater. Eng.* 302, 1–13.
  47. Cho, Y.H., Lee, I.H., and Cho, D.W. (2005). Laser scanning path generation considering photopolymer solidification in micro-stereolithography. *Microsyst. Technol.* 11, 158–167.
  48. Mayer, F., Richter, S., Westhauser, J., Blasco, E., Barner-Kowollik, C., and Wegener, M. (2019). Multimaterial 3D laser microprinting using an integrated microfluidic system. *Sci. Adv.* 5, eaau9160.
  49. Liu, Y., Lin, Y., Jiao, T., Lu, G., and Liu, J. (2019). Photocurable modification of inorganic fillers and their application in photopolymers for 3D printing. *Polym. Chem.* 10, 6350–6359.
  50. Goodridge, R.D., Shofner, M.L., Hague, R.J.M., McClelland, M., Schlea, M.R., Johnson, R.B., and Tuck, C.J. (2011). Processing of a polyamide-12/carbon nanofibre composite by laser sintering. *Polym. Test.* 30, 94–100.
  51. Dizon, J.R.C., Espera, A.H., Chen, Q., and Advincola, R.C. (2018). Mechanical characterization of 3D-printed polymers. *Addit. Manuf.* 20, 44–67.
  52. Chatham, C.A., Long, T.E., and Williams, C.B. (2019). A review of the process physics and material screening methods for polymer powder bed fusion additive manufacturing. *Prog. Polym. Sci.* 93, 68–95.
  53. Gibson, I., Rosen, D., Stucker, B., Gibson, I., Rosen, D., and Stucker, B. (2015). Material Jetting. In *Additive Manufacturing Technologies* (Springer), pp. 175–203.
  54. Truby, R.L., and Lewis, J.A. (2016). Printing soft matter in three dimensions. *Nature* 540, 371–378.
  55. Gibson, I., Rosen, D., Stucker, B., and Khorasani, M. (2021). Material jetting. *Addit. Manuf. Technol.* 203–235.
  56. Utela, B., Storti, D., Anderson, R., and Ganter, M. (2008). A review of process development steps for new material systems in three dimensional printing (3DP). *J. Manuf. Process.* 10, 96–104.
  57. Robertson, I.D., Yourdkhani, M., Centellas, P.J., Aw, J.E., Ivanoff, D.G., Goli, E., Lloyd, E.M., Dean, L.M., Sottos, N.R., Geubelle, P.H., et al. (2018). Rapid energy-efficient manufacturing of polymers and composites via frontal polymerization. *Nature* 557, 223–227.
  58. Shi, B., Shang, Y., Zhang, P., Cuadros, A.P., Qu, J., Sun, B., Gu, B., Chou, T.W., Fu, K., and Kelvin. (2020). Dynamic capillary-driven additive manufacturing of continuous carbon fiber composite. *Mater. Eng.* 2, 1594–1604.
  59. Shirai, M. (2015). Photoinitiated polymerization. In *Encyclopedia of Polymeric Nanomaterials*, Shiro Kobayashi, ed. (Springer Berlin Heidelberg), pp. 1579–1585.
  60. Li, J., Wu, C., Chu, P.K., and Gelinsky, M. (2020). 3D printing of hydrogels: rational design strategies and emerging biomedical applications. *Mater. Sci. Eng. R. Rep.* 140, 100543.
  61. Bahram, M., Mohseni, N., and Moghtader, M. (2016). An introduction to hydrogels and some recent applications. In *Emerging Concepts in Analysis and Applications of Hydrogels*, Sutapa Majee, ed. (InTech), pp. 9–38.
  62. Ahmed, E.M. (2015). Hydrogel: preparation, characterization, and applications: a review. *J. Adv. Res.* 6, 105–121.
  63. Chen, Z., Zhao, D., Liu, B., Nian, G., Li, X., Yin, J., Qu, S., and Yang, W. (2019). 3D printing of multifunctional hydrogels. *Adv. Funct. Mater.* 29, 1900971.

64. Ligon, S.C., Liska, R., Stampfl, J., Gurr, M., and Mühlaupt, R. (2017). Polymers for 3D printing and customized additive manufacturing. *Chem. Rev.* 117, 10212–10290.
65. Guvendiren, M., Lu, H.D., and Burdick, J.A. (2012). Shear-thinning hydrogels for biomedical applications. *Soft Matter* 8, 260–272.
66. GhavamiNejad, A., Ashammakhi, N., Wu, X.Y., and Khademhosseini, A. (2020). Crosslinking strategies for 3D bioprinting of polymeric hydrogels. *Small* 16, 2002931.
67. Ng, W.L., Goh, M.H., Yeong, W.Y., and Naing, M.W. (2018). Applying macromolecular crowding to 3D bioprinting: fabrication of 3D hierarchical porous collagen-based hydrogel constructs. *Biomater. Sci.* 6, 562–574.
68. Usta, M., Piech, D.L., MacCrone, R.K., and Hillig, W.B. (2003). Behavior and properties of neat and filled gelatins. *Biomaterials* 24, 165–172.
69. Bae, J., Li, Y., Zhang, J., Zhou, X., Zhao, F., Shi, Y., Goodenough, J.B., and Yu, G. (2018). A 3D nanostructured hydrogel-framework-derived high-performance composite polymer lithium-ion electrolyte. *Angew. Chem. Int. Ed.* 57, 2096–2100.
70. Guo, F., Aryana, S., Han, Y., and Jiao, Y. (2018). A review of the synthesis and applications of polymer-nanoclay composites. *Appl. Sci.* 8, 1696.
71. Sarkar, S., Guibal, E., Quignard, F., and SenGupta, A.K. (2012). Polymer-supported metals and metal oxide nanoparticles: synthesis, characterization, and applications. *J. Nanoparticle Res.* 14, 715.
72. Ramakrishna, S., Mayer, J., Wintermantel, E., and Leong, K.W. (2001). Biomedical applications of polymer-composite materials: a review. *Compos. Sci. Technol.* 61, 1189–1224.
73. Yang, H., Leow, W.R., Wang, T., Wang, J., Yu, J., He, K., Qi, D., Wan, C., and Chen, X. (2017). 3D printed photoresponsive devices based on shape memory composites. *Adv. Mater.* 29, 1701627.
74. Foo, C.Y., Lim, H.N., Mahdi, M.A., Wahid, M.H., and Huang, N.M. (2018). Three-dimensional printed electrode and its novel applications in electronic devices. *Sci. Rep.* 8, 1–11.
75. Chen, S., Wang, H.Z., Zhao, R.Q., Rao, W., and Liu, J. (2020). Liquid metal composites. *Matter* 2, 1446–1480.
76. Xin, A., Su, Y., Feng, S., Yan, M., Yu, K., Feng, Z., Lee, K.H., Sun, L., and Wang, Q. (2021). Growing living composites with ordered microstructures and exceptional mechanical properties. *Adv. Mater.* 33, 2006946.
77. Xia, Y., Zhou, P.Y., Cheng, X.S., Xie, Y., Liang, C., Li, C., and Xu, S.G. (2013). Selective laser sintering fabrication of nano-hydroxyapatite/poly-ε-caprolactone scaffolds for bone tissue engineering applications. *Int. J. Nanomedicine* 8, 4197–4213.
78. Shpichka, A., Osipova, D., Efremov, Y., Bikmulina, P., Kosheleva, N., Lipina, M., Bezrukov, E.A., Sukhanov, R.B., Solovieva, A.B., Vosough, M., et al. (2020). Fibrin-based bioinks: new tricks from an old dog. *Int. J. Bioprinting* 6, 1–14.
79. Yang, L., Cui, J., Zhang, L., Xu, X., Chen, X., and Sun, D. (2021). A moisture-driven actuator based on polydopamine-modified MXene/bacterial cellulose nanofiber composite film. *Adv. Funct. Mater.* 31, 2101378.
80. He, M., Zhao, Y., Wang, B., Xi, Q., Zhou, J., and Liang, Z. (2015). 3D printing fabrication of amorphous thermoelectric materials with ultralow thermal conductivity. *Small* 11, 5889–5894.
81. Boley, J.W., Van Rees, W.M., Lissandrello, C., Horenstein, M.N., Truby, R.L., Kotikian, A., Lewis, J.A., and Mahadevan, L. (2019). Shape-shifting structured lattices via multimaterial 4D printing. *Proc. Natl. Acad. Sci. U S A* 116, 20856–20862.
82. Khoo, Z.X., Teoh, J.E.M., Liu, Y., Chua, C.K., Yang, S., An, J., Leong, K.F., and Yeong, W.Y. (2015). 3D printing of smart materials: a review on recent progresses in 4D printing. *Virtual Phys. Prototyp.* 10, 103–122.
83. Mondal, S., and Hu, J.L. (2006). Temperature Stimulating Shape Memory Polyurethane for Smart Clothing (NISCAIR-CSIR).
84. Campbell, D., Lake, M.S., Scherbarth, M.R., Nelson, E., and Six, R.W. (2005). Elastic memory composite material: an enabling technology for future furlable space structures. In Collection of Technical Papers – AIAA/ASME/ASCE/AHS/ASC Structures, Structural Dynamics and Materials Conference (the American Institute of Aeronautics and Astronautics), pp. 6735–6743.
85. Wache, H.M., Tartakowska, D.J., Henrich, A., and Wagner, M.H. (2003). Development of a polymer stent with shape memory effect as a drug delivery system. *J. Mater. Sci. Mater. Med.* 14, 109–112.
86. Charlesby, A. (2016). *Atomic Radiation and Polymers: International Series of Monographs on Radiation Effects in Materials* (Pergamon press LTD.).
87. Singh, M., Haverinen, H.M., Dhagat, P., and Jabbour, G.E. (2010). Inkjet printing—process and its applications. *Adv. Mater.* 22, 673–685.
88. Cutkosky, M.R., and Kim, S. (2009). Design and fabrication of multi-material structures for bioinspired robots. *Philos. Trans. R. Soc. A Math. Phys. Eng. Sci.* 367, 1799–1813.
89. Vashist, A., Vashist, A., Gupta, Y., and Ahmad, S. (2014). Recent advances in hydrogel based drug delivery systems for the human body. *J. Mater. Chem. B*, 2, 147–166.
90. Bassil, M., Davenas, J., and El Tahchi, M. (2008). Electrochemical properties and actuation mechanisms of polyacrylamide hydrogel for artificial muscle application. *Sensors Actuators B Chem.* 134, 496–501.
91. Kaswala, A., Dubey, P.K., Neethu, T.M., Dubey, P.K., and Kaswala, A.R. (2018). Prospects and applications of hydrogel technology in agriculture. *Int. J. Curr. Microbiol. Appl. Sci.* 7, 3155–3162.
92. Crook, C., Bauer, J., Guell Izard, A., Santos de Oliveira, C., Martins de Souza e Silva, J., Berger, J.B., and Valdevit, L. (2020). Plate-nanolattices at the theoretical limit of stiffness and strength. *Nat. Commun.* 11, 1–11.
93. Zhang, X., Yao, J., Liu, B., Yan, J., Lu, L., Li, Y., Gao, H., and Li, X. (2018). Three-dimensional high-entropy alloy-polymer composite nanolattices that overcome the strength-recoverability trade-off. *Nano Lett.* 18, 4247–4256.
94. Pham, M.S., Liu, C., Todd, I., and Lerthanasarn, J. (2019). Damage-tolerant architected materials inspired by crystal microstructure. *Nature* 565, 305–311.
95. Meza, L.R., Zelhofer, A.J., Clarke, N., Mateos, A.J., Kochmann, D.M., and Greer, J.R. (2015). Resilient 3D hierarchical architected metamaterials. *Proc. Natl. Acad. Sci. U S A* 112, 11502–11507.
96. Wu, W., Qi, D., Liao, H., Qian, G., Geng, L., Niu, Y., and Liang, J. (2018). Deformation mechanism of innovative 3D chiral metamaterials. *Sci. Rep.* 8, 1–10.
97. Jiang, Y., and Li, Y. (2018). 3D printed auxetic mechanical metamaterial with chiral cells and re-entrant cores. *Sci. Rep.* 8, 1–11.
98. Vanneste, F., Goury, O., Martinez, J., Lefebvre, S., Delingette, H., and Duriez, C. (2020). Anisotropic soft robots based on 3D printed meso-structured materials: design, modeling by homogenization and simulation. *IEEE Robot. Autom. Lett.* 5, 2380–2386.
99. Do, A.V., Khorsand, B., Geary, S.M., and Salem, A.K. (2015). 3D printing of scaffolds for tissue regeneration applications. *Adv. Healthc. Mater.* 4, 1742–1762.
100. Wang, C., Huang, W., Zhou, Y., He, L., He, Z., Chen, Z., He, X., Tian, S., Liao, J., Lu, B., et al. (2020). 3D printing of bone tissue engineering scaffolds. *Bioact. Mater.* 5, 82–91.
101. Byambaa, B., Annabi, N., Yue, K., Trujillo-de Santiago, G., Alvarez, M.M., Jia, W., Kazemzadeh-Narbat, M., Shin, S.R., Tamayol, A., and Khademhosseini, A. (2017). Bioprinted osteogenic and vasculogenic patterns for engineering 3D bone tissue. *Adv. Healthc. Mater.* 6, 1–15.
102. Kang, H.W., Lee, S.J., Ko, I.K., Kengla, C., Yoo, J.J., and Atala, A. (2016). A 3D bioprinting system to produce human-scale tissue constructs with structural integrity. *Nat. Biotechnol.* 34, 312–319.
103. Zhao, C.Q., Liu, W.G., Xu, Z.Y., Li, J.G., Huang, T.T., Lu, Y.J., Huang, H.G., and Lin, J.X. (2020). Chitosan ducts fabricated by extrusion-based 3D printing for soft-tissue engineering. *Carbohydr. Polym.* 236, 116058.
104. Shen, K., Mei, H., Li, B., Ding, J., and Yang, S. (2018). 3D printing sulfur copolymer-graphene architectures for Li-S batteries. *Adv. Energy Mater.* 8, 1701527.
105. Fu, K., Wang, Y., Yan, C., Yao, Y., Chen, Y., Dai, J., Lacey, S., Wang, Y., Wan, J., Li, T., et al. (2016). Graphene oxide-based electrode inks

- for 3D-printed lithium-ion batteries. *Adv. Mater.* 28, 2587–2594.
106. Muth, J.T., Vogt, D.M., Truby, R.L., Mengüç, Y., Kolesky, D.B., Wood, R.J., and Lewis, J.A. (2014). Embedded 3D printing of strain sensors within highly stretchable elastomers. *Adv. Mater.* 26, 6307–6312.
107. Wu, S.Y., Yang, C., Hsu, W., and Lin, L. (2015). 3D-printed microelectronics for integrated circuitry and passive wireless sensors. *Microsyst. Nanoeng.* 1, 1–9.
108. Frutiger, A., Muth, J.T., Vogt, D.M., Mengüç, Y., Campo, A., Valentine, A.D., Walsh, C.J., and Lewis, J.A. (2015). Capacitive soft strain sensors via multicore-shell fiber printing. *Adv. Mater.* 27, 2440–2446.
109. Lopes, A.J., MacDonald, E., and Wicker, R.B. (2012). Integrating stereolithography and direct print technologies for 3D structural electronics fabrication. *Rapid Prototyp. J.* 18, 129–143.
110. Kong, Y.L., Tamargo, I.A., Kim, H., Johnson, B.N., Gupta, M.K., Koh, T.-W., Chin, H.-A., Steingart, D.A., Rand, B.P., and Mcalpine, M.C. (2014). 3D printed quantum dot light-emitting diodes. *Nano Lett.* 14, 7017–7023.
111. MacCurdy, R., McNicoll, A., and Lipson, H. (2014). Bitblox: printable digital materials for electromechanical machines. *Int. J. Robot. Res.* 33, 1342–1360. <https://doi.org/10.1177/0278364914532149>.
112. Bartlett, N.W., Tolley, M.T., Overvelde, J.T.B., Weaver, J.C., Mosadegh, B., Bertoldi, K., Whitesides, G.M., and Wood, R.J. (2015). A 3D-printed, functionally graded soft robot powered by combustion. *Science* 349, 161–165.
113. Yang, D., Mosadegh, B., Ainla, A., Lee, B., Khashai, F., Suo, Z., Bertoldi, K., and Whitesides, G.M. (2015). Buckling of elastomeric beams enables actuation of soft machines. *Adv. Mater.* 27, 6323–6327.
114. Wehner, M., Truby, R.L., Fitzgerald, D.J., Mosadegh, B., Whitesides, G.M., Lewis, J.A., and Wood, R.J. (2016). An integrated design and fabrication strategy for entirely soft, autonomous robots. *Nature* 536, 451–455.
115. Chen, T., Bilal, O.R., Shea, K., and Daraio, C. (2018). Harnessing bistability for directional propulsion of soft, untethered robots. *Proc. Natl. Acad. Sci. U S A* 115, 5698–5702.
116. Saha, S.K., Wang, D., Nguyen, V.H., Chang, Y., Oakdale, J.S., and Chen, S.C. (2019). Scalable submicrometer additive manufacturing. *Science* 366, 105–109.
117. Xiong, W., Liu, Y., Jiang, L.J., Zhou, Y.S., Li, D.W., Jiang, L., Silvain, J.-F., and Lu, Y.F. (2016). Laser-directed assembly of aligned carbon nanotubes in three dimensions for multifunctional device fabrication. *Adv. Mater.* 28, 2002–2009.
118. Sitthi-Amorn, P., Ramos, J.E., Wang, Y., Kwan, J., Lan, J., Wang, W., and Matusik, W. (2015). MultiFab: a machine vision assisted platform for multi-material 3D printing. In *ACM Transactions on Graphics (Association for Computing Machinery)*, pp. 1–11.
119. Choi, J.W., Kim, H.C., and Wicker, R. (2011). Multi-material stereolithography. *J. Mater. Process. Technol.* 211, 318–328.
120. Stephens, B., Azimi, P., El Orch, Z., and Ramos, T. (2013). Ultrafine particle emissions from desktop 3D printers. *Atmos. Environ.* 79, 334–339.
121. Kim, Y., Yoon, C., Ham, S., Park, J., Kim, S., Kwon, O., and Tsai, P.J. (2015). Emissions of nanoparticles and gaseous material from 3D printer operation. *Environ. Sci. Technol.* 49, 12044–12053.
122. Yang, Y., and Li, L. (2018). Total volatile organic compound emission evaluation and control for stereolithography additive manufacturing process. *J. Clean. Prod.* 170, 1268–1278.
123. Davis, A.Y., Zhang, Q., Wong, J.P.S., Weber, R.J., and Black, M.S. (2019). Characterization of volatile organic compound emissions from consumer level material extrusion 3D printers. *Build. Environ.* 160, 106209.
124. Pakkanen, J., Manfredi, D., Minetola, P., and Iuliano, L. (2017). About the use of recycled or biodegradable filaments for sustainability of 3D printing: state of the art and research opportunities. In *Smart Innovation, Systems and Technologies*, Robert Howlett, et al., eds. (Springer Science and Business Media Deutschland GmbH), pp. 776–785.
125. Zander, N.E., Gillan, M., and Lambeth, R.H. (2018). Recycled polyethylene terephthalate as a new FFF feedstock material. *Addit. Manuf.* 21, 174–182.